ESTABLISHING CANINE TRABECULAR MESHWORK CELL CULTURE

By

Hsiang-Rong Tsai

A THESIS

Submitted to
Michigan State University
in partial fulfillment of the requirements
for the degree of

Physiology - Master of Science

2016

ABSTRACT

ESTABLISHING CANINE TRABECULAR MESHWORK CELL CULTURE

By

Hsiang-Rong Tsai

Glaucoma is a leading cause of incurable blindness. The most common form of glaucoma is primary open-angle glaucoma (POAG) and is associated with pathological alterations of aqueous outflow facilities which lead to increased resistance and elevated intraocular pressure (IOP). Trabecular meshwork (TM) cells residing within the iridocorneal angle are considered key regulators of aqueous humor outflow; their malfunction is considered one of major factors in the pathogenesis of POAG. Glaucoma not only affects humans, but also other species such as dogs. Dogs are more accessible than other species to study the disease. Canine and human POAG share many features such as plaque formation within the TM with resulting slow progressive elevated IOP, and cupping of the optic nerve head. Because of the similarities between human and canine disease, we posit that the study of canine TM cells will be beneficial for the understanding of disease mechanisms in both dog and human. The purpose of this study was to establish primary canine TM cell cultures. Canine TM explants were carefully isolated and transferred to the cell culture dish. TM cells were identified by their expression of collagen type IV, alpha smooth muscle actin (α-SMA) and laminin, but not desmin and keratin. Another key feature of TM cells is their phagocytosis activity. Finally, the cultured TM cells form typical cross-linked actin networks (CLANs). To the best of our knowledge, this is the first report of primary canine TM (CTM) cultures.

ACKNOWLEDGEMENTS

I would like thank all individuals who supported my research and thesis writing, especially my colleagues, staff and professors from both the Department of Physiology and the College of Veterinary Medicine at Michigan State University.

First of all, I would like to appreciate my mentor Dr. András M. Komáromy. Like a lighthouse he provided me guidance for my research and professional life. His dedication for both research and clinical work provide me with an example about the life of a clinical scientist. Under his influence and encouragement, I have chosen to pursuit a degree in veterinary medicine at Michigan State University following my graduate work. I intend to dedicate my life to both research and clinical work with a hope to have a positive impact in this world. And I would like to thank my committee members Dr. Susanne Mohr and Dr. Arthur Weber who have given me constructive suggestion and guidance for my research. Special thanks to Dr. Susanne Mohr as director of the Physiology Graduate Program who guided both my graduate work and my career decision to pursuit a veterinary degree. I feel fortunate to have joined her program.

I would like to thank Mrs. Christine Herman, research associate, and Ms. Kristin Koehl, veterinary technician, for their full support of my research work. Without their kind support, I would not have been able to complete my research. I would also like to thank the following past members of the Komáromy Lab for their help and company: Forrest Nussdorfer, Josh Laske, and Gabriel Stewart.

Finally, I would like to thank my family members for their support, especially my parents and brother. Without their support, my pursuit of research would have been much harder. And I

want to thank the support from Taiwan through their generous scholarship and a grant from Midwest Eye-Banks to assist my study.

TABLE OF CONTENTS

LIST OF TABLES

LIST OF FIGURES

KEY TO ABBREVIATIONS

AAP	angular aqueous plexus
AH	aqueous humor
α-SMA	alpha-smooth muscle actin
CE	ciliary epithelium
CLAN	cross-linked actin network
CSTM	corneoscleral trabecular meshwork
CTM	canine trabecular meshwork
DAPI	4', 6-diamidino-2-phenylindole: DEX: Dexamethasone
ECM	extracellular matrix
FBS	fetal bovine serum
ICA	iridocorneal angle
ICC	immunocytochemistry
IOP	intraocular pressure
iPSCs	induced pluripotent stem cells
ISVP	intrascleral venous plexus
NPE	non-pigment epithelium
PACG	primary angle-closure glaucoma
PBS	phosphate-buffered saline
PE	pigmented epithelium
POAG	primary open-angle glaucoma
q-RTPCR	quantitative reverse transcription polymerase chain reaction

rAAV	recombinant adeno-associated virus
TGF-β2	transforming growth factor beta 2
TM	trabecular meshwork
UTM	uveal trabecular meshwork
wt	wild type

CHAPTER 1 – INTRODUCTION

Definition of glaucoma

Glaucoma is a leading cause of incurable blindness. It is defined as a progressive optic neuropathy characterized by the loss of retinal ganglion cells and clinically distinguishable cupping of the optic nerve head [1]. There are different forms of glaucoma, both primary and secondary, which all share the same risk factor of elevated intraocular pressure (IOP). This research is focused on primary glaucoma with no clinically observable underlying cause such as inflammation [2], neoplasia [3], or pigmentary dispersion [4]. The two most common forms of primary glaucoma are primary open-angle glaucoma (POAG) and primary angle-closure glaucoma (PACG). In both of these diseases, alterations along the aqueous humor (AH) outflow pathway result in increased resistance and IOP elevation (Fig. 1-1). While these changes are associated with closure of the iridocorneal angle (ICA) in PACG, the angle appears clinically normal and open in POAG [1]. In POAG, it is believed that the pathogenesis of disease is associated with molecular and cellular pathological changes in the trabecular meshwork (TM), a key regulator of AH outflow, resulting in impaired AH drainage from the eye. Those defects within the TM remain largely unknown.

Primary open-angle glaucoma (POAG)

POAG is considered a major type of glaucoma worldwide [5]. Elevated IOP is considered a major risk factor of POAG, but it can also develop without obvious IOP change, such as in 50% percent of European- and African- descent patients [6] and 92% for Japanese-descent patients [7,8].

In additional to IOP, several other POAG risk factors have been identified [9,10], such as aging, family history, and ethnicity.

Intraocular pressure (IOP): The level of IOP is the only risk factor which can be intervened by medical and surgical treatment [11]. In healthy individuals, the range of habitual IOP is 16.3 - 21.3 mmHg. In contrast, the IOPs of hypertensive POAG patients are usually over 22 mmHg [12]. In addition to being elevated, IOPs also fluctuates more in glaucomatous *vs*. normal eyes [12].

Aging: Both the incidence and prevalence of POAG strongly correlate with aging, especially after 40 years of age, due to gradual increase in AH outflow resistance [13]. For example, people of European-descent have a 25% incidence to develop POAG by the age of 64 years and up to 75% by 81 years [13]. A similar increasing age-related POAG incidence has also been observed in people of African-descent. Senescence of TM cells may contribute to this aging-related increase in AH outflow resistance [14]. Furthermore, aging seems to have a negative impact on the biomechanical properties of the eye: Elevated scleral stiffness associated with aging can result in increased stress and exacerbated IOP-related damage of the optic nerve head [15]. Finally, aging-related decrease of cerebrospinal fluid (CSF) pressure [16] may contribute to optic nerve head damage as well because of greater translaminar gradient [17].

Family history and genetics: Up to 50% of POAG patients have affected family members [18]. In addition, first degree relatives of an affected individual have a 22% risk to develop POAG *vs.* 2.3% risk in other family members [19]. This suggests that genetic predisposition is a critical risk factor of POAG development. The study of POAG-affected families not only identified high risk populations but also POAG candidate genes [20]. At least 7 genes have been associated with POAG: *MYOC* [21,22], *CYP1B1* [23], *WDR36* [24], *OPTN* [25,26], *LMX1B* [27], *NTF4* [28] and *ASB10* [29,30]

(Table 1-1). Other genes have been associated with POAG risk factors such as optic nerve head morphology, IOP and refractive error [31,32].

Table 1-1: Genes associated with POAG

Gene	Name	Location/Locus	Function	Reference
MYOC	**Myocilin, TIGR**	**1q23/ GLC1A**	**Cell migration, mitochondria, ECM turnover and cytoskeleton.**	**21,22**
CYP1B1	**Cytochrome P450 family 1**	**2p21/GLC3A**	**Metabolism of drug and lipid synthesis**	**23,33**
WDR36	**WD repeat domain 36**	**5q22/GLC1G**	**Ribosomal processes and cell growth**	**24,34,35**
OPTN	**Optineurin**	**10p14-p15/GLC1E**	**Rab-binding protein, TNF-alpha signaling NFkB pathway, immune response, apoptosis, vesicular transport, mitosis, cellular morphogenesis, oxidative stress protection.**	**25,36**
LMX1B	**LIM homeobox transcription factor 1-beta**	**9q34.1/NPS**	**Normal patterning of the dorsoventral axis, establishment of mid brain-hindbrain boundary, development of cerebellum and dopaminergic and serotonergic neurons.**	**27,37-39**
NTF4	**Neurotrophin-4**	**19q13.33/GLC1O**	**Survival and differentiation of mammal neurons, neurotrophin signaling pathway**	**28,40,41**
ASB10	**Ankyrin Repeat And SOCS Box Containing 10**	**7q35-q36/GLC1F**	**IOP regulation**	**29,30**

Ethnicity: The ethnicity was considered another important risk factor for glaucoma. For example, the study on African-derived population in the world-wide glaucoma epidemiology has consistently shown high prevalence of POAG compared with other populations [9,42-45].

Aqueous humor (AH) dynamics

The AH is a transparent medium that fills the anterior chamber located between iris and cornea. It does not only provide IOP to support the shape of the eye but also delivers nutrients and removes waste from the eyes [46]. In the normal eye, IOP is tightly regulated by well-coordinated production and outflow of AH [47]. In POAG-affected eyes, IOP can become elevated due to a dysregulation of the normal AH dynamics, especially an increase of outflow resistance through the TM – this is the main focus of our research. In the following paragraphs we will briefly discuss AH dynamics in the normal eye, before entering the detail of the POAG disease pathogenesis [48].

Aqueous humor formation

The ciliary body produces the AH. It can be subdivided in the *pars plicata* and *pars plana* which represent the anterior and posterior portion respectively. The ciliary epithelium (CE) of the *pars plicata* is the main location of AH production [49]. The CE covers the ciliary processes and is composed of two layers, the superficial non-pigment epithelium (NPE) and deep pigmented epithelium (PE). The basolateral surfaces of NPE cells face the posterior chamber while its apical surface forms gap junction to the counter part of the PE cells (arrow, Figure 1-1) [50]. The other side of the PE is in contact with the stroma of the ciliary process where solutes accumulate. In order to avoid blood protein and other inflammatory components to leak uncontrollably into the eye, the NPE cells form tight junction with neighbor cells; this is the blood-aqueous barrier [50].

In order to bring the nutrition from the blood to the eye, lipid-soluble and water soluble substances move via diffusion and ultrafiltration from the fenestrated capillaries across the ciliary stroma to the CE.

In the final stage of AH production, the solutes/substances are transported across the CE through diffusion, ultrafiltration and active transport. Among of them, active transport contributes about 80% to 90% of total AH formation [46,51]. Active transportation relies on the ion transporters [49]. The energy for active transportation is provided by hydrolysis of adenosine triphosphate (ATP) and mediated by Na^+-K^+-ATPase, which is mostly located in the NPE [50]. Besides Na^+-K^+-ATPase, NPE also requires carbonic anhydrase to secrete bicarbonate to regulate pH and maintain osmotic gradient for continuous AH secretion [52]. Carbonic anhydrase is an important target for glaucoma treatment: Inhibitor of carbonic anhydrase reduces AH production and thereby lowers IOP [53].

Aqueous humor outflow

IOP is regulated and maintained mainly by the conventional outflow [54]. Once the AH is formed, it flows from posterior chamber via pupil to the anterior chamber then drains through the ICA. AH outflow consists of conventional/trabecular and unconventional/uveosclera outflow. Unconventional outflow occurs via ciliary muscle and sclera, but is only responsible for <15% of AH outflow in the normal human eye [55]. In contrast, trabecular outflow provides the major drainage of AH and is regulated by the TM, a loose porous structure within the ICA (Figure 1-1.). The TM is composed by three components through which the AH has to drain: uveal, corneosclera and juxtacanalicular/ cribriform meshworks (Figure 1-1.) [56]. The pore size of the TM and AH flow rate are controlled by ciliary muscle tendons that are connected to an elastin

net within the juxtacanalicular TM [57]. Once it has passed through the juxtacanalicular meshwork, the AH enters the Schlemm's canal and through collector channels the episcleral veins and the systemic blood circulation. The circular Schlemm's canal is a unique structure that can only be found in human, primate and mouse [58-60], while other species such as dog [61], cat [62], pig [63], horse [64], rabbit [65] and zebrafish [66] have an angular aqueous plexus (AAP) instead to drain the AH.

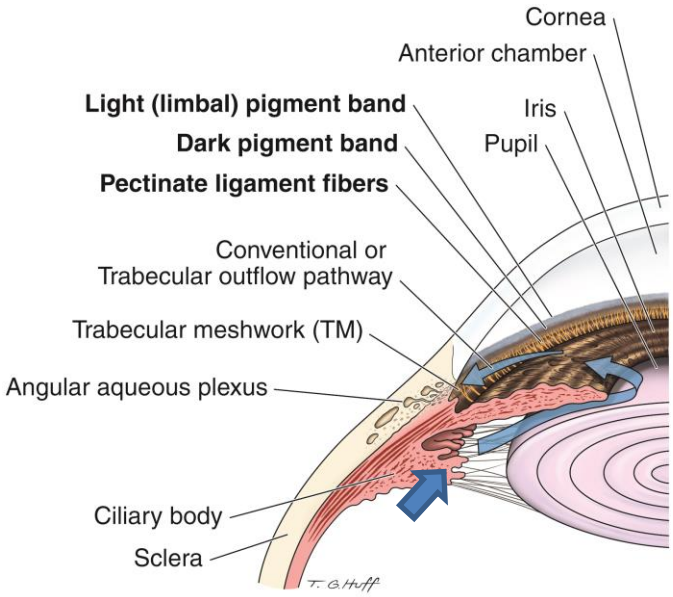

Figure 1-1 AH dynamics in the canine eye. The AH is formed and secreted by the CE covering the ciliary body (arrow). It drains through the TM and angular aqueous plexus within the ICA.

Physiology and pathophysiology of the TM

TM in normal eyes: The TM plays a critical role in regulating AH outflow and maintains the IOP in a normal range. It is derived from neural crest and cranial paraxial mesoderm [67]. There is increasing evidence that even once early differentiation is completed, a small population of progenitor cells reside within the TM and serve to replenish the loss of TM cells in the adult eye [68]. There is considerable evidence that the major AH outflow resistance is located in the

juxtacanalicular TM and the inner wall of Schlemm's canal [69]. This resistance is regulated by cellular and extracellular factors/components. The extra cellular matrix (ECM) production within the TM plays a major role in the resistance regulation [57]. Uveal and corneosclera TM form the beams of connective tissue or so called trabecular lamella which contain the core of elastic fibers and collagen surrounded by the sheaths [69]. These sheaths are formed by the TM cells, which highly express collagen type IV and laminin, important markers to characterize TM cells, while the core of the beams consist of collagen I and III [70,71]. The beams connect to each other in different layers of the TM to form porous filter-like structures. The thickness of beams increases with age, contributing to the increased POAG risk with age [69]. In contrast, the juxtacanalicular TM does not form beams of connective tissue but fibril elements of ECM instead. Juxtacanalicular TM cells and ECM fibrils together form an irregular network, the cribriform plexus which is lined against the inner wall endothelium of Schlemm's canal; this juxtacanalicular TM plays a major role in regulating the resistance of AH outflow [72]. Besides ECM turnover, the TM cells also have phagocytosis activity as a self-cleaning mechanism and to reduce/regulate the resistance of AH [73].

TM in POAG eyes: Both cellular and extracellular factors contribute to increased AH outflow resistance in POAG-affected eyes. ECM plaque formation and fibrosis have been found within the juxtacanalicular TM of POAG-affected eyes (Figure 1-2.) [57,74,75]. Furthermore, the TM cell structure appears to be altered in these eyes with increased formation of cross-linked actin networks (CLANs) [75]. The increased number of CLAN-positive TM cells results in increased cellular stiffness and contractility and higher AH outflow resistance [76]. Much effort has been put toward the investigation of the molecular pathways and growth factors involved in the cellular and extracellular changes within the TM [77]. Increased activation of transforming growth factor

beta 2 (TGF-β2) likely plays a major role since elevated concentrations can be found within the AH of POAG patients [78]. TGF-β2 also plays a major role in wound healing supporting its relevance in tissue fibrosis [79]. By increasing TGF-β2 in perfused human anterior chambers, outflow resistance increased and related ECM gene expression, such as fibronectin and plasminogen activator inhibitor-1, were also noticeably upregulated [80]. In addition, increased MYOC level in human POAG AH is considered another culprit for disease development within the TM [81].

Genetic predisposition and resulting altered gene expression is recognized as a critical factor within the glaucomatous TM (see also *Family history and genetics* above). Mutations in genes such as *Pax6* [82], *LTBP2* [83], *CYP1B1* [84], *MYOC* [85] affect the TM development and can lead to congenital glaucoma. The *MYOC* gene is considered a major POAG candidate gene [86]. Since *MYOC* is highly expressed in the TM, the hypothesis was raised that mutant *MYOC* accumulation within the TM results in TM malfunction and glaucoma [87]. Even though *MYOC* mutations are contributing to the pathogenesis of some forms of POAG and *MYOC* is highly expressed in glaucomatous TM cells, its major function remains unknown [88].

Current treatment options for POAG

Pharmacological approach: Current pharmacological therapies for POAG aim to either reduce AH formation or increase unconventional outflow (Table 1-2). For example, carbonic anhydrase inhibitors are used to inhibit the production of AH at the CE [89]. Prostaglandin analogs increase unconventional outflow [90]. Recently, a new class of glaucoma drugs has been developed, Rho-kinase inhibitors, which relax the TM and increase AH outflow [91].

Surgical approach: Surgical treatments focus on either reducing AH production or increasing AH outflow (Table 1-3). These include the use of lasers to partially destroy the ciliary processes in order to reduce AH production (cyclophotocoagulation) [92]. Trabeculoplasty or trabeculectomy directly target the TM to reduce the outflow resistance. Various types of shunts have been developed to facilitate AH outflow from the anterior chamber.

Table 1-2 and Table 1-3 summarize currently available therapies for POAG.

Table 1-2: Current therapies for POAG: Pharmacological therapies

Class	Mechanism	Available Drugs	Reference
Prostaglandin analogs	**Increase unconventional outflow via relaxation of the ciliary muscle and ECM remodeling in ciliary body**	**Latanoprost, Bimatoprost, Travoprost, Tafluprost, Unoprostone**	**90,93,94**
Beta-blockers	**Reduce AH production**	**Levobunolol, Carteolol, Metipranolol, Betaxolol, Timolol**	**94-96**
Alpha-agonists	**Constrict afferent ciliary process vasculature to reduce AH production; increase unconventional outflow**	**Brimonidine Tartrate, Dipivefrin hydrochloride, Apraclonidine hydrochloride**	**90,96-99**
Carbonic anhydrase inhibitors	**Reduce AH production**	**Brinzolamide, Dorzolamide**	
Miotics	**Contracting ciliary muscle and sclera spur to increase conventional outflow**	**Pilocarpine Hydrochloride, Carbachol, Echothiophate**	**89,90**

Table 1-2 (cont'd)			
Rho kinase inhibitor	**Inhibit the contraction of ciliary muscle and TM**	**Y-27632**	**100,101**
Hyperosmotics	**Reduce the volume of aqueous fluid**	**Glycerin, Mannitol**	**91,102,103**
Fix-combination	**Reduce AH production and elevate draining of AH outflow**	**Timolol maleate and Dorzolamide HCl, Brimonidine Tartrate and Timolol maleate, Brinzolamide and Brimonidine, Latanoprost and timolol, Bimatoprost and timolol, Travoprost and timolol.**	**104,105**

Table 1-3: Current therapies for POAG: Surgery therapies

Type of surgery	Mechanism	Duration	Reference
Laser cyclophotocoagulation	**Destroy ciliary processes to reduce AH production**	**IOP remains normal after 2 years from surgery**	**92,111,112**
Argon laser trabeculoplasty	**Targeting pigmented and non-pigmented TM cells but preserve architecture of TM to improve drainage**	**44% of eyes maintain normal IOP after 2 years from surgery**	**92,113**
Trabeculectomy	**Excise TM tissue to increase AH outflow**	**46.9% failure after 5 years from surgery**	**114,115**
Tube shunt	**Insert the tube through TM to Schlemm's canal or anterior chamber to increase outflow**	**29.8% failure after 5 years from surgery**	**115**

Animal models of POAG

Glaucoma is not only a human disease but also can be observed in other species. Animals with primary glaucoma provide us with a chance to study disease mechanisms in more detail and may present potential platforms to evaluate novel therapies development. In addition to these spontaneous diseases, experimental and transgenic animal models have also been developed to facilitate POAG study (Table 1-4). Induced ocular hypertension via episcleral vein in experimental animal model was applied to imitate elevated IOP environment of POAG and induce similar clinical phenotypes as POAG [116]. However, as previous paragraph, it should be noticed that ocular hypertension is not always associated with pathogenesis of POAG and is not used to determine POAG in clinical diagnosis but considered as major risk factor of POAG [1]. The approach of establishing experimental model by using induced ocular hypertension is to overcome the scarcity of spontaneous model and the sample of patients. It is similar but not as equal as the samples from spontaneous model and patients.

Table 1-4 lists some of the established animal models for POAG and ocular hypertension.

Table 1-4: Animal models of POAG & ocular hypertension

Species	Type of animal model	Mechanism	Clinical phenotype	Reference
Monkey	**Spontaneous**	**Inherited**	**POAG**	**117**
	Induced	**Laser photocoagulation of TM**		**118**
	Induced	**Intracameral injection of latex microspheres**		**119**
Dog	**Spontaneous**	**Inherited, *ADAMTS10* mutation**	**POAG**	**120,121**
Cat	**Spontaneous**	**Inherited, *LTBP2* mutation**	**POAG**	**122,123**

Table 1-4 (cont'd)				
Sheep	**Induced**	**Glucocorticoids induction**	**Ocular hypertension**	**[124]**
Cow	**Induced**	**Glucocorticoids induction**	**Ocular hypertension**	**[125]**
Rabbit	**Induced**	**Glucocorticoids induction**	**Ocular hypertension**	**[126]**
Rat	**Induced**	**Episcleral vein injection with hypertonic saline**	**POAG**	**[116]**
Mouse	**Transgenic**	***MYOC* mutation**	**POAG**	**[127]**
Mouse	**Transgenic**	***OPTN* mutation**	**POAG**	**[128]**
Mouse	**Transgenic**	**α1 subunit of collagen Type 1 mutation**	**Ocular hypertension**	**[129]**
Zebrafish	**Transgenic**	***Lrp2* mutation**	**POAG**	**[130]**

In vitro model systems of POAG

Although animal models provide us unique opportunities to observe and study disease mechanisms, there are downsides, including the need to sacrifice animals and the high housing expenses. Moreover, species differences may prevent direct translation of findings from animals to humans. *In vitro* systems that have been developed to study AH outflow pathways include TM cell cultures (Table 2-1) and anterior ocular segment perfusion culture which has been successfully developed on human [131] and bovine [132]. These systems allow the use of human surgical TM tissue samples or whole donor eyes.

Rational for studying canine glaucoma and TM

Many purebred dogs have a genetic predisposition for primary glaucoma with prevalence comparable or higher than humans; commonly affected dogs breeds include American Cocker Spaniel (5.52%), Basset Hound (5.44%), Chow Chow (4.70%) and Shar-Pei (4.40%) [133]. Dogs with primary glaucoma, including POAG, provide us with a unique opportunity to study its pathogenesis. The best established canine glaucoma model is inherited POAG in beagle dogs [134]. Its clinical relevant phenotype for human POAG include the slow progressive, sustained IOP elevation [135], response to glucocorticoid challenge [136], cupping of the optic nerve head [134], and plaque formation within the TM [57,137] (Figure 1-2). Compared with other species, dogs are more accessible and have similar anatomical ocular features as humans, such as similar globe size, TM structure and response to topical IOP-lowering medication [134,136,138-140]. Moreover, recent successful developments of ocular recombinant adeno-associated virus (rAAV) mediated gene therapy in dogs were translated into human clinical trials, such as for Leber congenital amaurosis [141] and achromatopsia [142]. This explains our interest in canine models of glaucoma, including the study of canine TM cells.

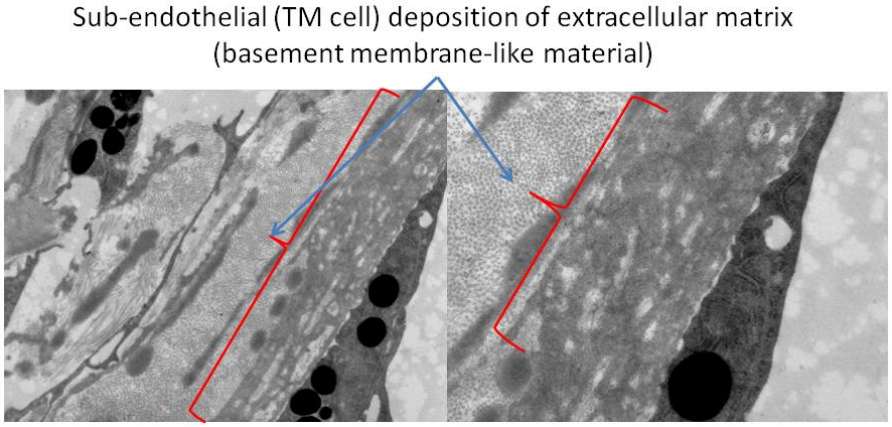

Figure 1-2 ECM accumulation in the TM of POAG-affected dogs.

In addition, glaucomatous dogs represent a source of tissue for the study of disease mechanisms. Although primary human TM cell cultures are well established, the size of the trabeculectomy specimens is usually small [74]. This increases the difficulty to isolate and culture sufficient TM cells, especially when considering the limited numbers of passages [74]. Whole eyes from human donors with well-established history and clinical data are rare and difficult to obtain.

To the best of our knowledge, there are no published reports on the development of primary canine TM cell cultures. Thus, there is a need to develop and characterize primary canine TM cell cultures; this was the purpose of this study.

CHAPTER 2 – METHODS

Isolation of the canine TM (CTM)

17 canine eyes from 9 adult dogs were collected within 5 minutes of euthanasia. These were either dogs from a local animal shelter or research dogs euthanized for reasons unrelated to this study. The globes were stored on ice until further processing. The 5 eyes from 3 dogs obtained from the shelter were used to refine the steps of tissue dissection and histologic identification of tissue types. The 12 eyes obtained in the laboratory were used to harvest and culture TM cells within 20 hours of enucleation (Table 3-1). The procedures were approved by the Michigan State University IACUC, and were done in accordance with the ARVO Statement for the Use of Animals in Ophthalmic and Vision Research.

The surfaces of the globes were aseptically prepared with 10% povidone iodine and 70% ethanol, then rinsed with 1X working concentration phosphate-buffered saline, pH 7.4 (PBS). The posterior segment was removed from the anterior segment by cutting the globe along the pars plana of the ciliary body with a No. 11 scalpel blade and Westcott tenotomy scissors (Figure 2-1). The lens was then removed from the anterior segment by cutting the lens zonules with Westcott tenotomy scissors (Figure 2-1). The ciliary body and iris were bluntly dissected from the sclera in a posterior to anterior direction (Figure 2-1). The TM tissue could then be recognized as a white band on the ciliary body, delimited anteriorly by the pectinate ligament (Figure 2-1). The identification of the TM was confirmed histologically by processing the dissected tissue routinely for paraffin embedding, sectioning, and staining with hematoxylin and eosin (H&E) (Figure 2-1). Sections were electronically scanned and analyzed by using the Aperior ScanScope slide scanner and software (Leica Microsystems Inc., Buffalo Grove, IL, USA). Only a small trace of juxtacanalicular TM tissue remained connected to the sclera along a

pigmented line (Figure 2-1). The TM could be isolated and separated from uveal tract by sharp dissection of the white band (Figure 2-1).

Figure 2-1 Dissection procedure. The globe was first dissected to separate the anterior from the posterior segment (A & B). The ciliary body and iris were separated from the sclera (C). The clear white TM band could be identified on the surface of the ciliary body (C, arrowhead). The white band was carefully dissected from the ciliary body and cut into small pieces for primary culture (D, arrowhead). Histologic evaluation of the dissected tissue confirmed the successful isolation of the TM: Only traces of the corneoscleral TM (CSTM) and uveal TM (UTM) remained connected to the sclera and ciliary body respectively (E,F, G, narrow arrowhead). And

angular aqueous plexus (AAP) can be seen clearly besides remnant CSTM and was connected to the intrascleral venous plexus (ISVP). The histologic appearance of the isolated explants was consisted with TM (H, narrow arrowhead).

Primary TM cell culture

Once the TM was isolated, we followed previously described methods for other species to establish primary cultures [143]. TM tissue was carefully cut in approximate 3x3mm square pieces using Westcott tenotomy scissors. Each piece was placed separately in a 15.6-mm diameter well (24-well Costar™ Cell Culture Plates, Corning, Tewksbury, MA) containing 500 µl of low glucose Dulbecco's Modified Eagle's Medium (DMEM) (Sigma-Aldrich, St. Louis, MO) with 1% penicillin/streptomycin (Sigma-Aldrich), 10% fetal bovine serum (FBS) (Atlas, Fort Collins, CO) and 1% L-glutamine (Thermo Fisher Scientific, Waltham, MA) [143].

Within 2 weeks the cells migrated from the tissue onto the bottom surface of the well. The shape of TM cells may vary slightly between species but can generally be described as oval to elongated (see Results) in contrast to spindle-shaped fibroblasts [144-147]. Furthermore, TM cells have a unique overlapping-pattern [144-147].

The medium was replaced every 7 days in order to avoid a more frequent interruption of the cell migration process. Once the cells in the well reached confluency within 2-3 weeks, they were detached from the bottom of the well together with the TM tissue remnant with a1x working concentration of trypsin (Thermo Fisher Scientific), re-suspended, and transferred in 5 mL of medium to a T-25 tissue culture flasks (Corning) for passage as previously described [144]. The culture medium was then changed every 48 hours until the cells reached confluency, then

they were passaged again into three T-75 tissue culture flasks (Corning). After reaching confluency within 7-10 days, the cells were counted and used for either analyses of cell properties (immunocytochemistry (ICC), CLAN quantification, phagocytosis assay and DEX challenge) or long-term storage (Figure 2-2). Long-term storage was done by cryopreservation: Cells were suspended in cryopreservation medium which contained 10% cell culture quality dimethyl sulfoxide (Sigma-Aldrich) and 90% DMEM (Sigma-Aldrich).The cell numbers were determined with a hemocytometer (Thermo Fisher ScientificA). Then the cell suspension was transferred to 1ml cryovials (USA Scientific, Inc., Ocala, FL) with a concentration of 10^6 cells /ml. Cryovials were then transferred into a cell freezing container with 100% isopropyl alcohol (Thermo Fisher Scientific) and kept in a -80℃ freezer (Thermo Fisher Scientific) overnight. Then the cryovials were moved into a liquid nitrogen tank (Thermo Fisher Scientific) for long-term storage.

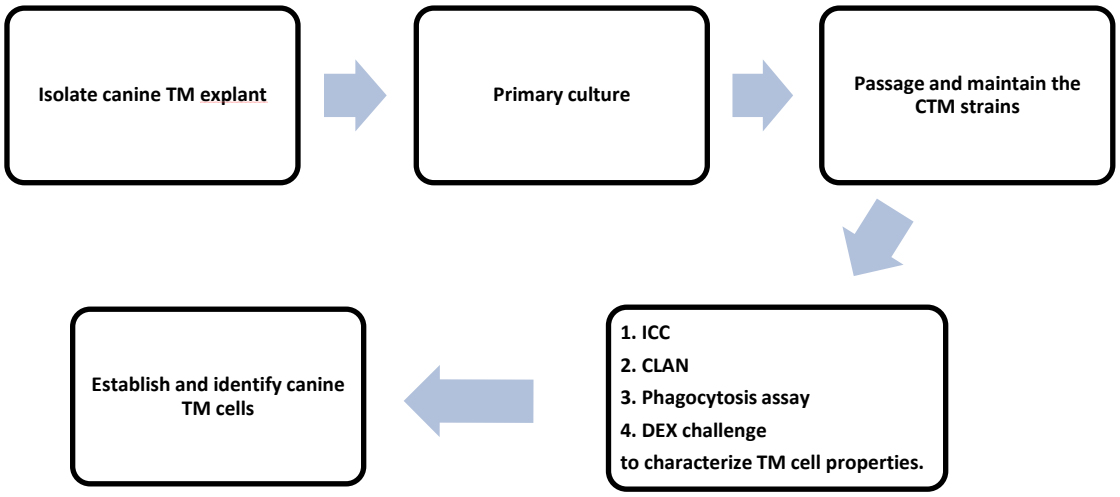

Figure 2-2 Experimental design.

Fibroblast primary culture

Primary fibroblast cell cultures were obtained from wild type (*wt*) canine skin samples concurrently with eye collection and use as negative controls to compare with primary CTM cultures. In the selected area, the hair was removed with clipper and the skin was aseptically prepared with 70% ethanol and 4% chlorhexidine. Skin samples were then collected with a 4-mm biopsy punch (Acuderm inc., Fort Lauderdale, FL). The procedure of fibroblast isolation was previous described [148,149]. Briefly, the skin tissue was aseptically prepared with 70% ethanol and then washed with PBS. Then the tissue was cut into small pieces and each piece was placed separately into the wells of a 6-well receiver plate with poly-D-lysine coating (Millipore, Billerica, MA). DMEM-high glucose medium with 10% FBS and 1% Antibiotic-Antimycotic containing penicillin, streptomycin, and amphotericin B (Thermo Fisher Scientific) was prepared for culture and replaced every 7 days. Once the cells reached confluency, they were treated with trypsin for passage and expansion in T-25 tissue culture flasks (Corning) and subsequent cryopreserved for future experiments. When needed for different experimental purposes, the cells were passaged to T-75 tissue culture flasks (Corning) after reaching confluency in the T-25 tissue culture flasks.

Characterization of TM cells – ICC

Characterizing TM cells was challenging due to lack of a single specific TM cell marker. Rather we had to rely on a combination of different cell markers to identify TM cells; these have been well-established in other species [144-147]. TM cells highly express collagen type IV, laminin and alpha-smooth muscle actin (α-SMA) [144-147] (Table 2-1). Other markers such as desmin and keratin were also introduced to exclude other types of cells such as corneal epithelium and ciliary

smooth muscle cells. Increased expression of myocilin and CLAN formation with DEX stimulation are other TM-specific features.

For ICC, the cells were cultured in the Nunc Lab-Tek II Chamber Slide System (Thermo Fisher Scientific, MA) with seeding density 0.05 x 10^6 cell number per well until day reached confluency. After approximate 7 days, routine immunostaining and DEX challenge were performed. The cells were fixed in 4% paraformaldehyde for 30 minutes and then washed with 0.25% Triton-X100/1X working concentration PBS, pH 7.4. The cells were then incubated overnight at 4℃ with primary antibodies (Table 2-2) [144]. Secondary antibodies were applied for 1 hour at room temperature (Table 2-2). Finally, Phalloidin/ F-actin AF488 1:100 (Thermo Fisher Scientific) was added and incubated at room temperature for 1 hour to stain the F-actin network in the cells. ProLong Gold Antifade Mountant with 4',6-diamidino-2-phenylindole (DAPI) (Life Technologies, Carlsbad, CA) was added to the slides before covered with coverslips. The slides were imaged and evaluated with epi-fluorescent microscopy (Eclipse 80i Fluorescent Microscope, Nikon Instruments Inc., NY) and confocal microscopy (FV1000 Laser Scanning Confocal Microscope, Olympus America Inc., PA).

Table 2-1: Characterization methods previously used for TM cell identification.

Species	Morphology description	Characterization methods	Reference
Human	**Monolayer formation, cobblestone pattern, fast grow after P8**	**ICC DEX challenge**	**150**
Human	**Endothelium-like monolayer**	**ICC, DEX challenge, phagocytosis assay, CLAN formation.**	**145,151-156**
Primate	**Basement membrane, intercellular junction, pinocytotic vesicles, microvillous projections, and branched cell extension and monolayer growth pattern.**	**Radiolabeling, DEX challenge, phagocytosis assay**	**157-159**
Porcine	**Monolayer**	**ICC Southern hybridization Western blot**	**160**
Mouse	**Similar morphology as HTM cells**	**ICC DEX challenge CLAN formation Phagocytosis assay**	**147,161**
Bovine	**Morphology similar as human TM cells**	**ICC DEX challenge CLAN formation**	**143,144**

Table 2-2: The list of antibodies used in the experiments

Antibody	Type	Host Species	Concentration	Manufacturer
α-SMA	Monoclonal	Mouse	1:500	BioGenex, Fremont, CA
Laminin	Polyclonal	Rabbit	1:250	Sigma-Aldrich, St. Louis, MO
Collagen type IV	Polyclonal	Rabbit	1:50	LS Bioscience, Seattle, WA
Cytokeratin	Monoclonal	Mouse	1:50	Invitrogen, Carlsbad, CA
Desmin	Monoclonal	Mouse	1:100	Cell Marque, Rocklin, CA
Phalloidin/ F-actin AF488	Dye	None	1:100	Thermo Fisher Scientific, Waltham, MA
Anti-rabbit IgG conjugated with Texas Red	Polyclonal	Goat	1:1000	Thermo Fisher Scientific, Waltham, MA
Anti-mouse IgG conjugated with Texas Red	Polyclonal	Goat	1:5000	Thermo Fisher Scientific, Waltham, MA

Characterization of TM cells - Phagocytosis assay

The TM cells were first cultured in Nunc Lab-Tek II Chamber Slide System (Thermo Fisher Scientific). Then, E-coli conjugated pHrodo green particles (0.5 mg/well, Invitrogen) were added and incubated for 1 hour at 37 ℃. Those particles remain non-fluorescent outside the cells at neutral pH but emit green fluorescence once engulfed in phagosomes with an acidic pH. Therefore, by observing green fluorescent particles within the cultured cells, we could confirm phagocytosis activity [162]. The cells were fixed in 4% paraformaldehyde and co-stained with F-actin to verify the cell structure and location. The slides were coverslipped with ProLong Gold Antifade Mountant with DAPI. Epi-fluorescence microscopy (Eclipse 80i Fluorescent Microscope, Nikon Instruments Inc) was used to observe and co-localize the cells and engulfed particles to verify phagocytosis activity.

Dexamethasone (DEX) challenge

In order to verify that our isolated cell strains consist of TM cells, they were treated with DEX as previous described and briefly outlined below [163]. Unique characteristics of TM cells are the up-regulation of myocilin mRNA and protein as well as the increased formation of cross-linked actin networks (CLANs) following treatment with DEX [164]. CLANs are defined as geodesic structures composed of at least 3 triangles with 5 hubs [143,163]. This arrangement is considered to increase the stiffness of TM cells, resulting in elevated AH outflow resistance *in vivo* following treatment of POAG-affected eyes with DEX [75].

Induction of myocilin mRNA: Confluent TM cells were cultured in 6-well plates and treated for 3 days with either 100 nM DEX (Sigma-Aldrich, MO) or 0.1% ethanol as vehicle

control in DMEM-high glucose medium with 1% penicillin/streptomycin, 10% FBS, and 1% L-glutamine. DEX was first dissolved in ethanol and prepared as 10^{-3} M stock solution before treatment and therefore ethanol was selected as vehicle control. Approximately 10^6~10^7 cells were used for both treatment groups to extract total RNA with RNeasy Mini Kit (Qiagen, Venlo, Netherland) following manufactures instructions. Briefly, cells were harvested as a cell pellet and mixed with 350 μl of lysis buffer. Next, 70% ethanol was added to the lysate and filtered through a RNeasy Mini spin column. Then the column was washed with washing buffer. Finally, RNA was eluted with 30 μl RNase-free water and collected for quantification with a Nanodrop ND-1000 Spectrophotometer (Thermo Fisher Scientific). Only the samples with 260nm/280nm ratio of ~ 2.0 or above were considered as pure RNA and accepted for future experiments. The extracted RNA was then treated with DNase (Roche, Basel, Switzerland) to eliminate potential host genome contamination. Reverse transcription of mRNA to cDNA was performed with Superscript II (Invitrogen) with the addition of oligo dT (Life Technologies), 10 mM dNTP (Invitrogen, CA), 0.1M DTT (Invitrogen), and RNase OUT (Invitrogen). The TaqMan probes and primers for canine myocilin (Cat# Cf02627377_m1, Applied Biosystems, Waltham, MA) and the housekeeping gene 18s (Cat# Hs99999901_s1) were used for quantitative-RTPCR (q-RTPCR). mRNA extracted from canine TM tissue was used as positive control for canine myocilin expression [165].

q-RTPCR was performed on a 7500 Fast Real-Time PCR system (Applied Biosystems) using 50 ng cDNA for each sample. cDNA was mixed with 1 μl primer /probes and 10 μl TaqMan Fast Universal Master Mix 2X (Thermo Fisher Scientific) then added up with DNase-free water to 20 μl total volume. Relative gene expression for each gene was compared with house keeper gene based on the equation $1/[2\hat{}(Ct_{target\ gene} - Ct_{housekeeper})]$ and $\Delta\Delta$Ct method was

applied for group comparison. Briefly, the Ct value of *MYOC* mRNA was normalized with 18s to give ΔCt value for each group. To calculate the difference ΔΔCt, the ΔCt value of ethanol treated group was subtracted from the ΔCt value of the DEX treated group. ΔΔCt was used to calculate relative fold changes of gene expression ($2^{-\Delta\Delta Ct}$) [166].

CLAN quantification: Confluent TM cells cultured in Nunc Lab-Tek II Chamber Slide System (Thermo Fisher Scientific) for ICC were treated for 10 days with either 100 nM DEX (Sigma-Aldrich) or 0.1% ethanol as vehicle control in DMEM-high glucose medium with 1% penicillin/streptomycin, 10% FBS, and 1% L-glutamine. The medium was replaced every other day. At post-treatment day 10, the cells were collected and fixed with 4% paraformaldehyde. Phalloidin/ F-actin AF488 (Thermo Fisher Scientific) was added and incubated at room temperature for 1 hour to stain the cellular F-actin network. Finally, the slides were coverslipped with ProLong Gold Antifade Mountant with DAPI (Life Technologies). All slides for CLAN formation were evaluated with confocal microscopy (FV1000 Laser Scanning Confocal Microscope, Olympus America Inc., PA) and images were taken at 10x, 20x, 40x, and 60x magnification. For CLAN quantification, five regions in each well of the chamber slides with approximately 50-230 cells per region were imaged with confocal microscopy (FV1000 Laser Scanning Confocal Microscope, Olympus America Inc.) at 20x. The CLAN formation rate was estimated by the ratio of CLAN-positive cells and total number of cells with DAPI staining. The cells were counted in double-blind fashion as previously describe [144]. Then the CLANs formation rate was compared between DEX and ethanol treated cells with student's t-test Only $P<0.05$ was considered significant.

CHAPTER 3 – RESULTS

Histological evaluation of isolated CTM explant

Although human and canine ocular anatomy are similar, there are some unique structures within the canine ICA, such as the pectinate ligament and AAP. These slight anatomic differences resulted in the need to develop the methods for TM isolation specifically for the dog. As described under Methods, we performed several dissections of canine cadaver eyes with histologic evaluations to verify isolation of the canine TM (Figure 2-1).

In summary, the CTM was effectively dissected from the uveal tract, and we confirmed histologically that our procedure successfully isolated TM tissue from the sclera and ciliary body. In Table 3-1, we provide the list of established CTM cell strains.

Table 3-1: Established primary CTM cell strains

Canine Participant	Eye	Gender	Age(months)	Cell strain	ICC	Phagocytosis	DEX-CLAN	DEX-MYOC	Passage number
BER01	**OS**	**F**	**10.4**	**BERTM2B**	**Y**	**Y**	**ND**	**ND**	**2**
BER01	**OD**	**F**	**10.4**	**BERTM7A**	**Y**	**Y**	**Y**	**ND**	**5**
BER01	**OS**	**F**	**10.4**	**BERTM7B**	**Y**	**Y**	**ND**	**ND**	**6**
BER01	**OS**	**F**	**10.4**	**BERTM8B**	**Y**	**Y**	**Y**	**Y**	**6**
BER01	**OS**	**F**	**10.4**	**BERTM5B**	**Y**	**ND**	**ND**	**ND**	**2**
BER01	**OD**	**F**	**10.4**	**BERTM1A**	**Y**	**ND**	**ND**	**ND**	**2**
BER01	**OD**	**F**	**10.4**	**BERTM3A**	**Y**	**ND**	**ND**	**ND**	**2**
BOST01	**OS**	**F**	**1.1**	**BOSTM1B**	**Y**	**Y**	**Y**	**ND**	**5**
BOST01	**OD**	**F**	**1.1**	**BOSTM2A**	**ND**	**Y**	**ND**	**ND**	**1**
BOST01	**OS**	**F**	**1.1**	**BOSTM2B**	**ND**	**Y**	**ND**	**ND**	**2**
BOST01	**OD**	**F**	**1.1**	**BOSTM3A**	**ND**	**Y**	**ND**	**ND**	**2**
BOST01	**OS**	**F**	**1.1**	**BOSTM3B**	**ND**	**Y**	**ND**	**ND**	**3**
BOST01	**OS**	**F**	**1.1**	**BOSTM4B**	**ND**	**Y**	**ND**	**ND**	**2**
R01	**OD**	**M**	**2.8**	**ROYTM3A**	**ND**	**ND**	**Y**	**ND**	**6**
R01	**OS**	**M**	**2.8**	**ROYTM3B**	**ND**	**ND**	**ND**	**ND**	**4**
R01	**OD**	**M**	**2.8**	**ROYTM4A**	**ND**	**ND**	**ND**	**ND**	**4**
R01	**OS**	**M**	**2.8**	**ROYTM4B**	**ND**	**ND**	**ND**	**ND**	**4**
R01	**OS**	**M**	**2.8**	**ROYSCTM**	**ND**	**ND**	**ND**	**ND**	**6**
R01	**OS**	**M**	**2.8**	**ROYCRTM**	**ND**	**ND**	**ND**	**ND**	**4**
TEL01	**OD**	**M**	**2.8**	**TELTM8A**	**ND**	**ND**	**ND**	**ND**	**4**
TEL01	**OS**	**M**	**2.8**	**TELTM8B**	**ND**	**ND**	**ND**	**ND**	**4**
CUR01	**OD**	**F**	**9.4**	**CURTM3A**	**ND**	**ND**	**ND**	**ND**	**11**
CUR01	**OS**	**F**	**9.4**	**CURTM3B**	**ND**	**ND**	**ND**	**ND**	**4**
CUR01	**OD**	**F**	**9.4**	**CURTM4A**	**ND**	**ND**	**ND**	**ND**	**4**
CUR01	**OS**	**F**	**9.4**	**CURTM4B**	**ND**	**ND**	**ND**	**ND**	**4**
HOU01	**OD**	**M**	**2.7**	**HOUTM1A**	**ND**	**ND**	**ND**	**ND**	**6**
HOU01	**OS**	**M**	**2.7**	**HOUTM1B**	**ND**	**ND**	**ND**	**ND**	**4**
HOU01	**OD**	**M**	**2.7**	**HOUTM2A**	**ND**	**ND**	**ND**	**ND**	**4**

Table 3-1 (cont'd)

HOU01	**OS**	**M**	**2.7**	**HOUTM2B**	**ND**	**ND**	**ND**	**ND**	**4**

OS: oculus sinister; OD: oculus dexter; F: Female; ND: not done; Y: done

The migration of TM cells onto the culture plate was noticed within 2 weeks after culturing the explanted tissues (Figure 3-1). These cells continued to expand until they reach confluency within additional 7 to 10 days. The growth pattern of CTM cells was similar as described in other species with features of overlapping cell growth and cobble-stone like monolayer appearance (Figure 3-1) [164,167]. The morphology of canine TM cells appeared flat with enlarged intracellular spaces; this has also been observed in the cultured human TM cells [168].

The TM cells that were isolated from adult canine eyes could be successfully passaged at least up to 6 times, although the cells failed to reach confluency and became senescence after passage 5. This phenomenon is consistent with other published results [150,169] and possibly affected by the age of donors. Human TM cells from adult donors have fewer passage numbers and longer population doubling times compared to human fetal TM cells [150,169].

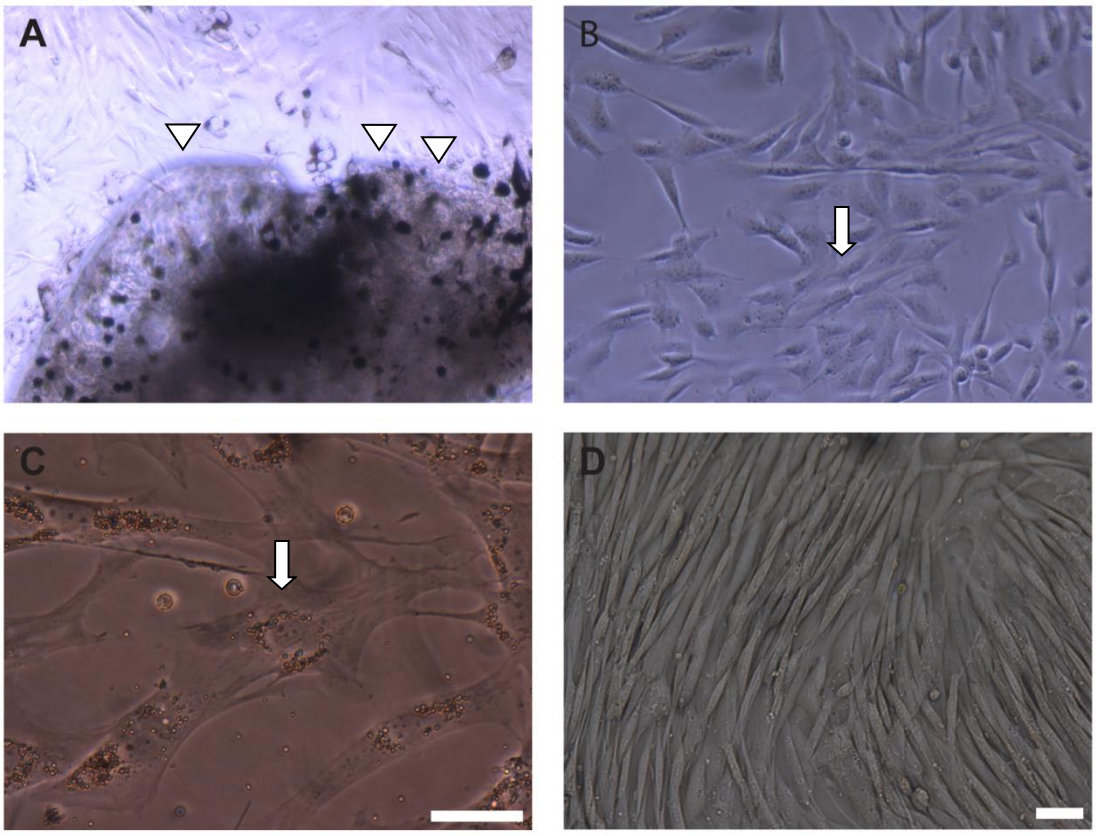

Figure 3-1 Cell migration and morphology of canine TM cells and fibroblasts. Cell migration from the TM tissue onto the culture plate was noticed within 2 weeks (1A, arrow head). The newly migrated cells had overlapped pattern and cobble stone-like monolayer (1B, arrow). The small vacuoles around the nucleus suggest phagocytoses activity (1C, arrow). Canine fibroblasts are shown for comparison (1D); compared to TM cells fibroblasts have less intercellular space, and they have a more elongated shape. (calibration bars = 50 μm)

Characterization of cultured TM cells: Immunocytochemistry

Since there is no specific marker for TM cells, we used combined markers as previously described to identify the cultured canine TM cell strains [167,170]. In here, we present the results from 8 different established CTM cell strains and 1 canine fibroblast cell strain which is BERFB01 as negative control. The confluent canine TM cells express α-SMA which can be clearly seen in the cytoplasm with filamentous pattern. This is consistent with the previous results of an IHC study of canine ICA [171]. Although the age of the canine can affect α-SMA expression in the TM tissue [171], our CTM cell strains strongly express α-SMA. Similarly, laminin and collagen type IV stain intracellular vesicles but not the extracellular space of cultured cells (Figure 3-2). No keratin or desmin was observed in the CTM cell strains which indicated there were no cornea epithelium cells and ciliary smooth muscle cells, respectively (Figure 3-2). Table 3-2 summarizes the result of our canine cell strain characterization.

Table 3-2: Characterization of canine cell strains

Cell strain	Collagen Type IV	Laminin	α-SMA	Desmin	Keratin
BERTM7B	+	+	+	(+)	-
BERTM8B	+	+	+	(+)	-
BERTM5B	+	+	+	-	-
BERTM2B	+	+	+	-	-
BERTM7A	+	+	+	-	-
BERTM3A	+	+	+	-	-
BERTM1A	+	+	+	-	-
ROYTM3A	+	+	+	-	-
BOSTM1B	+	+	+	-	-
BERFB01	-	-	-	-	-

+: positive; -: negative; (+): slightly desmin-positive cells observed; BERFB01 is fibroblast

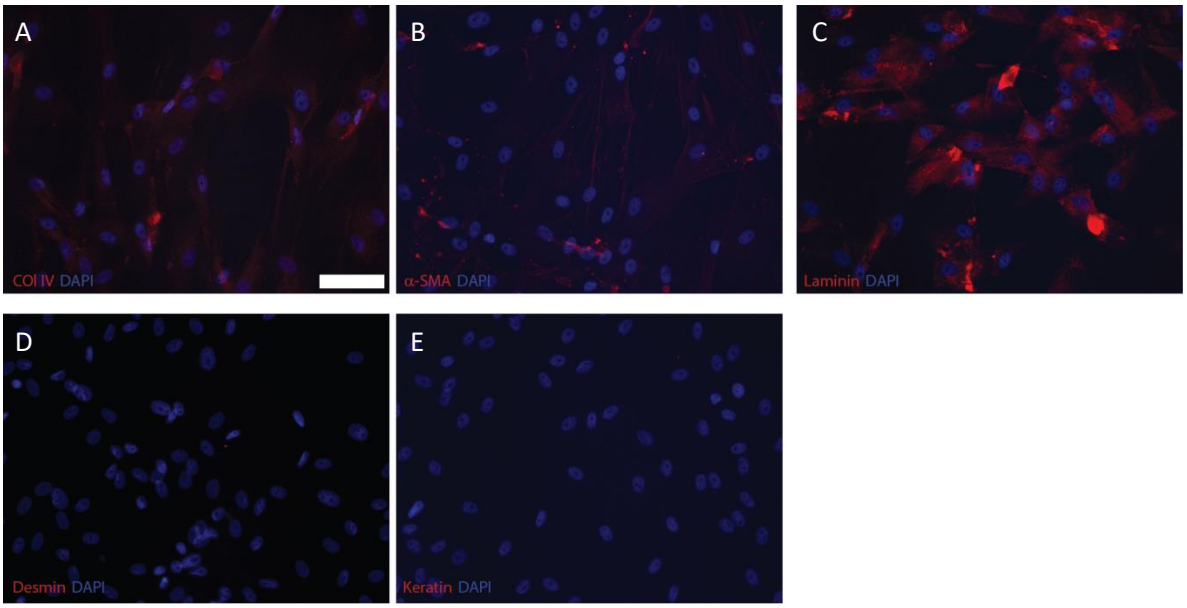

Figure 3-2 The ICC result of CTM. ICC staining shows positive expression of collagen IV (A), laminin (C) and α-SMA (B) in red, but no expression of desmin (D) and keratin (E). This staining pattern is consistent with TM cells. (Calibration bar = 50 μm)

Characterization of cultured TM cells: Phagocytosis assay

In addition to light microscopic observations and ICC, we also performed phagocytosis assays to verify the TM characteristics of our cultured cells. Phagocytosis is considered an important function of TM cells to clear debris within the TM in order to maintain aqueous humor outflow [172-174]. Our first observed indication of phagocytosis activity was localization of pigment particles in some of the cells (Figure 3-3). For confirmation, we incubated the cells for 1 hour with acid-sensitive E-coli conjugated pHrodo green particles. When the green particles were engulfed into phagosomes, they become green fluorescent and can be detected by epifluorescence microscopy. We demonstrated that our cultured cells had phagocytosis activity further confirming them to be TM cells (Figure 3-3).

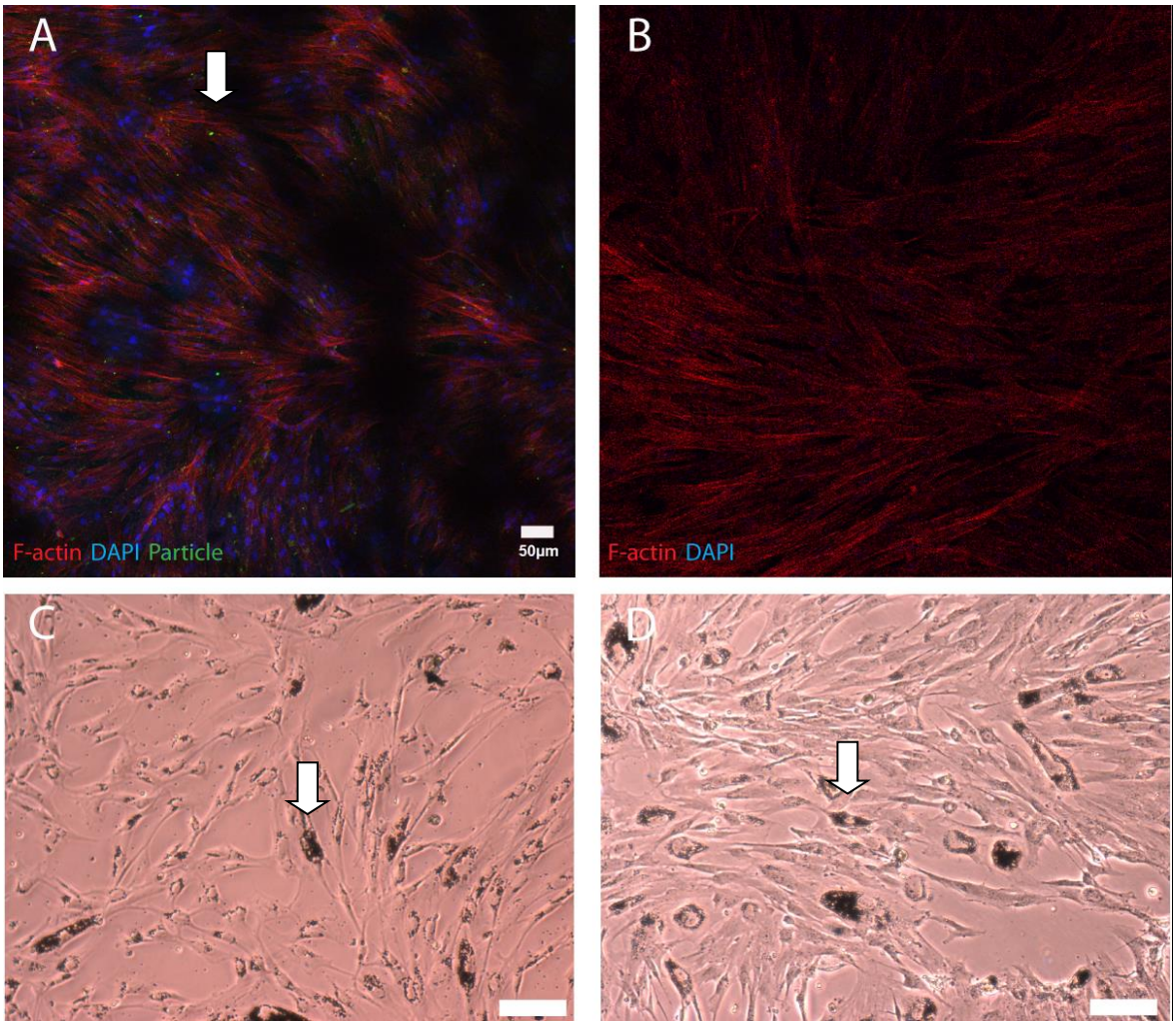

Figure 3-3 Phagocytosis activity of cultured CTM cells. After 1 hour incubation with green fluorescent particles, phagocytosis activity of CTM was observed with particles engulfed clearly in the intracellular space of cells overlapped with F-actin (3A, arrow shows one of many engulfed particles). In comparison, canine fibroblasts did not show any phagocytosis activity (3B). Indications for phagocytosis activity were also observed in unstained, untreated primary TM cell cultures by pigment engulfed in cells. (Arrow, 3C&3D) (calibration bar = 50 μm)

Table 3-3: Phagocytosis activity of canine cell strains

Cell strain	Pigment engulfed	Green particle engulfed
BERTM7A	-	+
BERTM7B	-	+
BERTM8B	-	+
BOSTM4B	+	ND
BOSTM3B	+	ND
BOSTM2B	+	ND
BOSTM1B	+	+
BOSTM3A	+	ND
BOSTM2A	+	ND
BERFB01	-	-

-: not observed, +: observed; ND: not done; BERFB01: canine fibroblast

Characterization of cultured TM cells: DEX challenge - CLAN formation

The promotion of CLAN formation after DEX challenge is considered one of critical features of many TM cells [143,145]. Such induction was rarely observed in other cell types [175]. Therefore, we were interested whether cultured *wt* CTM cells will increase CLAN formation after DEX treatment [143,147,164].

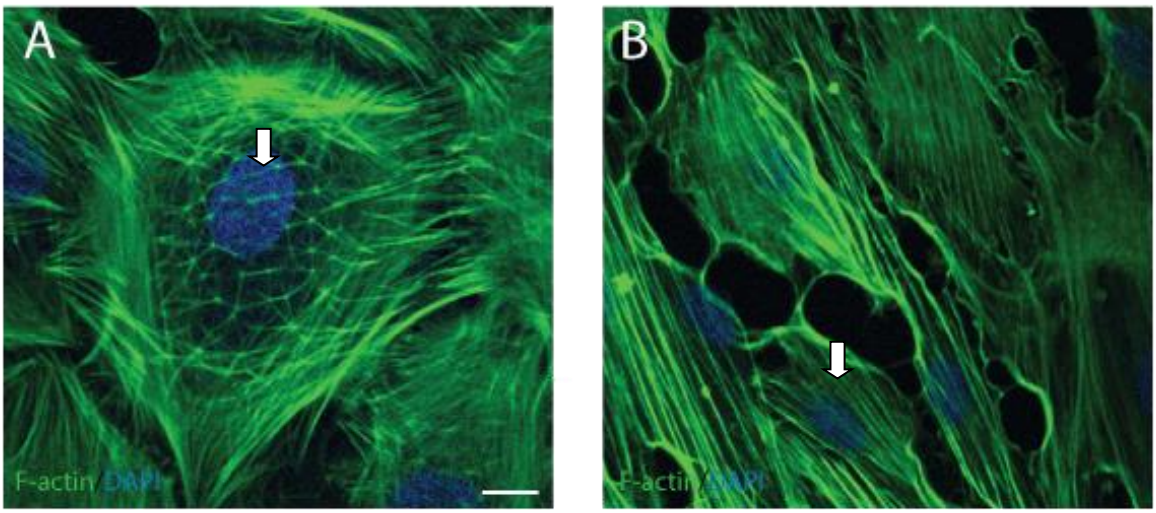

Figure 3-4 CLAN formation in canine TM cells. CLANs could be observed in some cultured CTM cells with and without DEX treatment (4A, arrow) but not in fibroblasts. (4B, arrow) The

structure is similar as previously reported with hub and triangle structure. (calibration bar = 10 μm)

In order to determine DEX-induced upregulation of CLAN formation, we counted CLAN-positive cells of CTM cells following 10 days of DEX treatment and compared them to cells treated with ethanol vehicle control. Ethanol was used as solvent for DEX. Canine fibroblasts were included as negative controls since there are no reports about CLAN formation in this cell type [175]. The slides were evaluated with confocal microscopy and 5 cell strains including 3 CTM cell strains (BERTM7A, BERTM8B, BOSTM1B) and 1canine fibroblast strain (BERFB01) were used in this experiment for CLAN evaluation (Figure 3-5). Five regions in each well of the chamber slides with approximately 50-230 cells per region were imaged and counted. However, after 10 days of DEX treatment, we didn't observe an increase in the number of CLAN positive cells. Additionally, we didn't find CLANs in the CTM cells under normal culture condition. Student's t test was performed to evaluate the result of CLANs number after treatment. There was no significant difference between DEX-treated and ethanol-treated groups ($P > 0.05$, Figure 3-5). We counted 3±1% CLANs-positive cells (mean ± SD) in BER7ATM, 1±1% in BER8BTM and 1±1% in BOS1BTM following DEX treatment while cells treated with ethanol have 4±3% CLANs-positive cells in BER7ATM, 1±1% in BER8BTM and 1±1% in BOS1BTM. Consistent with previous reports, this suggests that F-actin was altered in our cultured CTM cells [75,143,147], but the effect of DEX challenge was not obvious to be reflected on the number of CLANs.

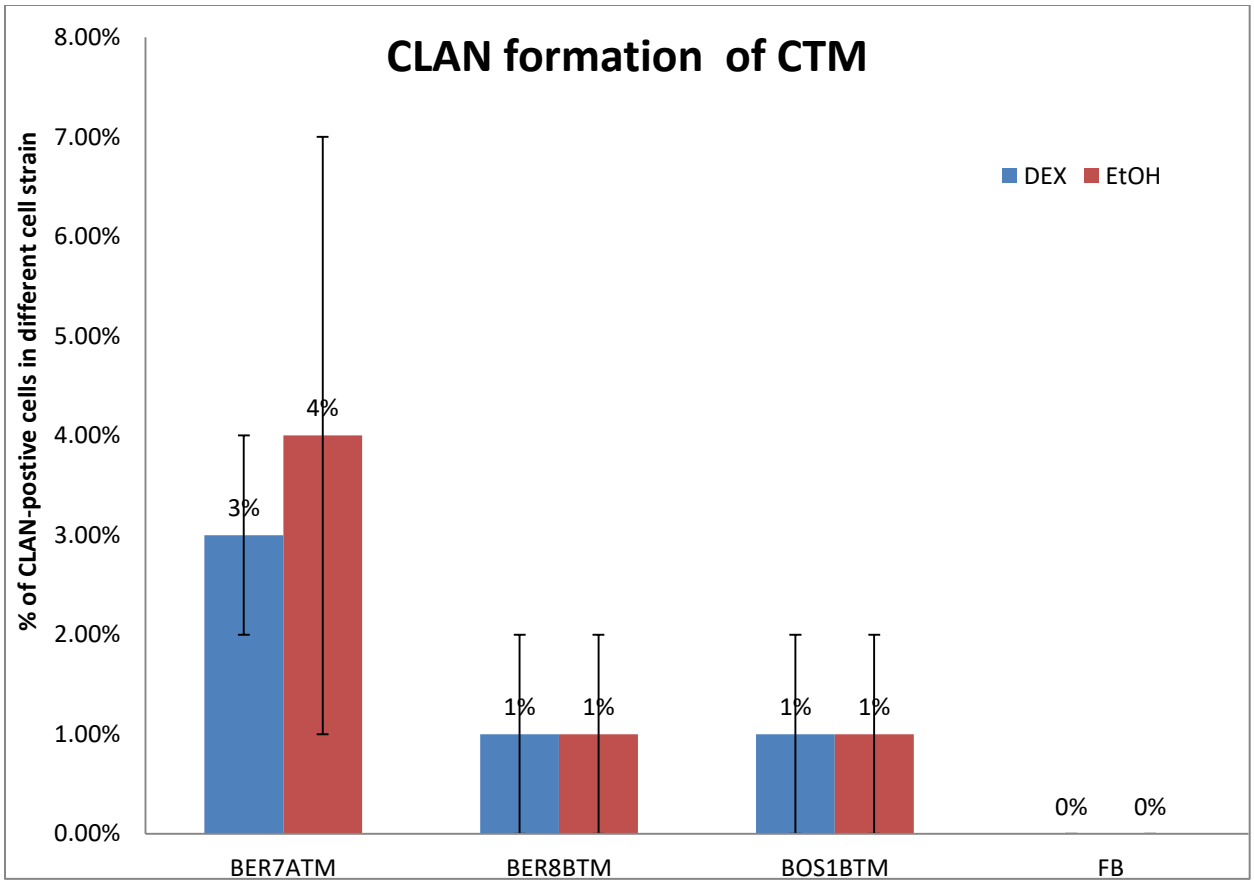

Figure 3-5 Relative number of CLAN-positive cells in different canine cell strains. (mean ± one SD) DEX: DEX treatment, EtOH: Ethanol treatment, FB: fibroblast. *P* value for BER7ATM is 0.36, for BER8BTM is 0.72, and for BOS1BTM is 0.91. The result was shown there is no significant difference between DEX-treated group and ethanol vehicle control group.

Characterization of cultured TM cells: DEX challenge – gene expression

In order to verify gene expression, we performed q-RTPCR of CTM cells cultured with ethanol vehicle control or DEX treatment (Figure 3-6 & Table 3-6). One of the characteristics of many TM cells strains is the upregulation of *MYOC* expression with DEX treatment [144].

Our result showed a decreased rather than increased myocilin expression following the DEX treatment. However, the sample size is small and additional experiments needed to be

performed. In BER8BTM, the fold expression of *MYOC* was 0.0002 while in BER7ATM it was 0.76 following DEX treatment (Figure 3-6).

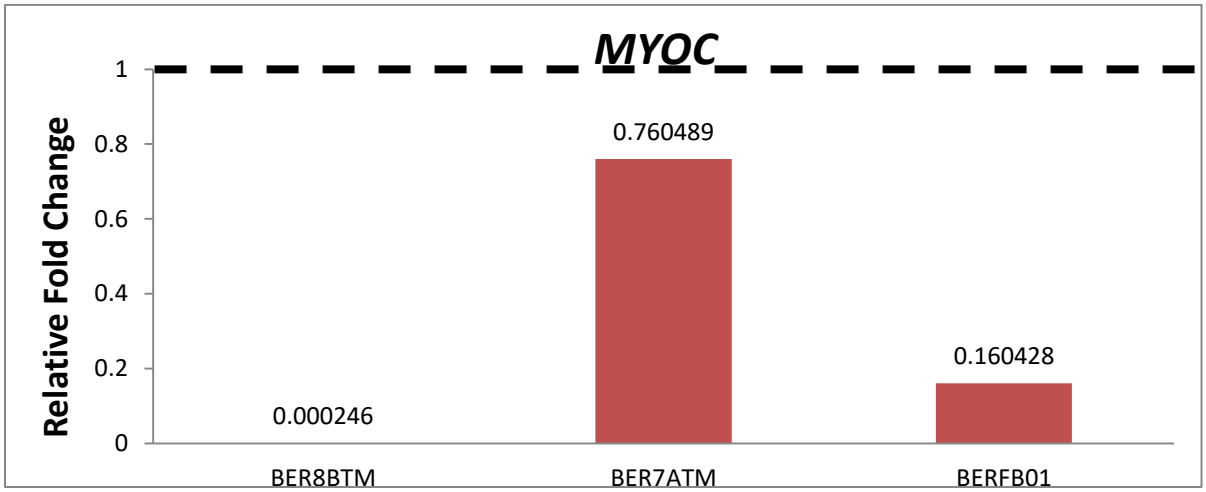

Figure 3-6 Relative gene expression of *MYOC* following 3 days of DEX treatment in different canine cell strains. The fold changes were variable across CTM cell strains but indicated a decreased *MYOC* expression. There was 0.0002 fold expression in BER8BTM while BER7ATM had a 0.76 fold change.

Table 3-4: Completed q-RTPCR of CTM cell strains and other type of cells

Canine participant	Gender	Age (months)	Cell strain	Treatment	Target genes	Amplification	△△Ct	Housekeeping genes
BER01	F	10.4	7ATM	DEX/EtOH	*MYOC*	Y	0.76	18S
BER01	F	10.4	8BTM	DEX/EtOH	*MYOC*	Y	0.0002	18S
BER01	F	10.4	FB01	DEX/EtOH	*MYOC*	Y	0.16	18S

F: Female; M: *MYOC*; Y: has amplification

CHAPTER 4 – DISCUSSION

To the best of our knowledge this is the first report of the successful isolation and culture of CTM cells. We have identified several well-established TM-cell properties in our primary CTM cell strains, such as phagocytosis activity, expression of α-SMA, laminin and collagen type IV, and CLAN formation.

Most TM tissue was excised for cell culture as confirmed by histologic examination

Performing resection of small TM tissue pieces has always been considered a challenge whether for surgery [176,177] or primary culture [74,147,150]. Isolating TM tissue without excising other type of tissue is critical to establishing CTM cell strains. Only traces of TM tissue remained attached to the sclera and ciliary body after isolation, according to histologic examination. This suggested the success of TM isolation and reduced the concern of mixing cell types in the cell culture. A few pigmented cells, presumed uveal melanocytes, were observed in the culture dish together with the TM cells. However, from published reports of culturing canine uveal melanocytes, the cell culture medium and supplements for TM cells are not suitable to maintain uveal melanocytes [178]. Those pigmented cells lacking the proper culture conditions would not survive after replacing the medium several times. As such, we didn't observe those cells after 1 - 2 passages.

Multiple TM-specific protein markers are observed at our TM cell strains

Our CTM cells did express the TM specific proteins mentioned in previously published reports in other animal species [143,147]. Because there is no specific marker for TM cells, the

expression of a combination of multiple proteins had to be characterized in order to confirm that our cultured cells are indeed TM cells. Following the well-established protocol developed by others, we used the following five antibodies to identify our TM cells by ICC: laminin, α-SMA, collagen IV, keratin and desmin [144]. TM cells express laminin, α-SMA and collagen IV but not keratin and desmin. Based on this staining pattern, we are confident that we successfully cultured CTM cells.

CLAN formation observed in our non-DEX treated CTM cells

CLAN formation is an important characteristic of TM cells [145]. Other ocular cells that have been reported to form CLAN include lamina cribrosa cells [179], human and bovine retinal pigment epithelium, rabbit lens epithelium, bovine corneal endothelium and bovine iris pigment epithelium [175]. But based on the anatomic location and our dissection technique, it is unlikely that we cultured any of these other cell types. Corneal endothelial cells could have been cultured, but we excluded this possibility based on cell morphology and positive α-SMA stain. This suggests that the CLAN formation we observed occurred in CTM cells.

A low percentage of CLAN-positive cells could be observed under DEX untreated conditions, which has been reported before [143]. DEX promotes CLAN formation but CLAN-positive cells also exist under non-DEX treated conditions. Our result has shown ~1 -4% CLAN-positive cells without DEX treatment which is consistent with previous publications [143,163].

Phagocytosis activity of the CTM cells

One of the important phenomena observed during our primary culture of CTM cells was phagocytosis activity. TM cells perform phagocytosis in order to remove debris and reduce the

resistance of trabecular AH outflow. Presumed phagocytic vesicles were observed in our cultured cells once they migrated from the tissue explants into the culture plate; this was consistent with previously published reports [180]. Moreover, functional phagocytosis activity was confirmed by incubating the cultured cells with bio-particles; these particles could be clearly seen inside the cells, again consistent with previously published reports [162,173].

CTM cells didn't have significant DEX response

We did observe clear CLAN structures after DEX treatment in our CTM cells. However, this could also be seen in the EtOH-treated control group, and no significant difference in the number of CLANs was observed. Approximately 1-4% of cultured CTM cells were CLAN-positive even after 10 days of DEX treatment. This is in contrast to other species, such as human [145], bovine [143] and mouse [147] where an increase in CLAN positive cells can be observed following DEX treatment. The result of human TM cells has shown that around 18- 55% of CLAN-positive cells appear after 10 days DEX treatment [145], while in bovine an estimated 40% of DEX-treated TM cells were observed with CLAN structure [143]. Approximately 30% of cultured murine TM cells were CLAN-positive with DEX treatment [147]. We suspect that the induction of CLAN-formation by DEX in cultured TM cells correlates with a particular species' IOP-responsiveness to DEX (see explanation below).

Similarly, we did not observe an increase in *MYOC* mRNA expression following DEX treatment. Our q-RTPCR results indicated a slight difference but not large fold changes as previously published [181-184]. However, when evaluating published results more closely, it became clear that not all TM cells respond to DEX treatment, especially cells harvested from normal human eyes [146]. Only 38.1% to 52.1% of normal human TM cells responded to DEX treatment

with an increased expression of the MYOC protein [146]. Moreover, we noticed that *MYOC* mRNA expression is hard to detect even following DEX treatment. It is possible that our PCR probe will have to be redesigned. The current probe is used effectively to measure *MYOC* RNA levels in tissue. However, we assume that the quantity of harvested cells for q-RTPCR is much less than in the tissue samples. This is the first time we have applied canine *MYOC* probes in cell culture. We suspect we will need more sensitive probe or increase the amount of cells used in the experiment. In the future, we will also quantify *MYOC* protein expression by Western blot as complement to our q-RTPCR experiments.

It is possible that species differences should be considered in order to interpret our data properly. DEX-induced ocular hypertension can been seen in normal cattle [125], sheep [124] and mouse [185]. However, based on our clinical experience and previous publications, the majority of *wt* dogs are non-responders [186]. Considering that *wt* dogs do not respond to topical DEX treatment with an increase in IOP, it is rational that we did not observe a change in CLAN formation and *MYOC* expression in our *wt* canine TM cells. It remains to be shown if TM cells from glaucomatous *ADAMTS10*-mutant dogs respond to DEX since IOP increases in these animals with topical DEX treatment [136].

The concern of inadvertently isolating non-TM cells

We did our best to exclude other, non-TM tissues during the dissection, and we histologically confirmed our isolated TM explants. However, we cannot rule out the possibility that other cell types were isolated along with the TM tissue, such as fibroblasts [187,188], sclera spur cells [189], and ciliary smooth muscle cells [190]. In the future we may use additional antibodies to verify in more detail the presence of other cell types by ICC.

Senescence observed in the CTM cell strains

We observed that the time of reaching cell confluency was gradually increased after several passages. Limited passage number of TM cells ranging from 2 to 6 passages has been noticed during cell culture. The phenomenon of TM cell senescence has been reported in several species. Human TM cells have been reported to stop proliferation after 8 to 12 passages [170]; and porcine TM cells have been shown to become flat and senescence at passage number 8 [169]. Primary bovine TM cells reached senescence after about 10 passages [144]. Similar results have also been recorded for murine TM cells, which can proliferate until passage number 25 before reaching senescence [147]. Compared with other species, with the exception of mice, our results on CTM cell passage number do not appear different. Primary TM cells can reach senescence in early passages due to the quality of the cells or the age of the donor.

It has been suggested that senescence of TM cells *in vivo* may contribute to increase in trabecular outflow resistance in the POAG pathogenesis [191]. It remains to be shown if cultured TM cells from canine glaucomatous eyes develop senescence at earlier passage numbers than *wt* CTM cells. A possible solution to prevent senescence of cultured TM cells is their transfection with mutant defective SV40 virus [170], which can be included in our future investigations.

CHAPTER 5 - SUMMARY AND FUTURE DIRECTIONS

Summary

This study documents the first successful isolation and culture of CTM cells. These cells were characterized based on their ability to perform phagocytosis and their expression of α-SMA, laminin and collagen type IV, but not keratin and desmin [75,143,144,147]. Moreover, we observed CLAN formation, an alteration of F-actin that is somewhat specific for TM cells, since CLANs are rarely seen in other cells types [175]. In summary, all our presented data is consistent with the published results on cultured TM cells from other species.

Our primary cultured *wt* CTM cell cultures did not respond to DEX treatment. This is consistent with our clinical experience: *wt* dogs, in contrast to some humans [192] and bovines [125], do not respond to DEX treatment with an increase in IOP. In contrast, *ADAMTS10*-mutant beagles with POAG have shown such an IOP response to topical DEX treatment [136]. Nonetheless, DEX-induced upregulation of *MYOC* expression [87] and increased CLANs formation [143,145,147] are considered hallmarks of many TM cell strains.

Future directions

The tools developed here can be applied in the detailed study of disease mechanisms involved in canine primary glaucoma, which is a leading cause of incurable blindness. Primary CTM cultures from glaucomatous eyes will provide us with a unique opportunity to study disease mechanisms without the secondary effects of elevated IOP and therapy. We consider this a valuable alternative option to study human TM cells due to the scarcity of glaucomatous human donor eyes. The investigation of CTM from *wt* and glaucoma-affected eyes will likely assist in providing a better understanding of both canine and human disease.

Whether glaucomatous CTM cells can be successful established remains to be shown, one of the initial challenges to isolate CTM from eyes with advanced stages of glaucoma is the scarcity of TM tissue, due to the presumed loss of TM cells affected by chronically elevated IOP [193]. This scarcity of glaucomatous TM tissue may increase the difficulty in isolating and maintaining enough number of TM cells for experiments. We have launched initial attempts to isolate TM cells from *ADAMTS10*-mutant dogs with advanced POAG with promising results.

We performed some additional preliminary gene expression analyses by evaluating *ADAMTS10*, a gene that has previously been shown to be highly expressed in the TM [120]. However, we didn't find conclusive result on our established *wt* CTM cell strains [120]. ADAMTS10 is a metalloproteinase responsible for ECM turnover. It may play a major role in the regulation of ECM production within the TM. Mutation of *ADAMTS10* can decrease ECM turnover and thus contribute to the elevated resistance of AH outflow as seen in *ADAMTS10*-mutant humans [194] and dogs with POAG [120]. However, the role of *ADAMTS10* in the pathogenesis of POAG remains largely unknown, and therefore we would like to further investigate its role in our glaucomatous CTM cells in the future.

The comparison of cultured CTM cells from *wt* and glaucoma affected dogs will include the evaluation of gene and protein expression patterns in order to determine up- or downregulation of particular pathways, such as profibrotic factors (e.g., TGFβ2) and collagens, and possible epigenetic effects. Moreover, we are interested how the difference in gene expression in the glaucomatous CTM cells affects their biomechanical properties [195].

From our previous research, the alteration of sclera collagen microstructure in the posterior chamber led to the weakness of sclera was noticed in *ADAMTS10*-mutant dogs with advanced POAG [196]. It appears that age-associated weakness of the sclera can increase the severity of the

damage to the optic nerve leading to an increase in the progression of the disease. Similar biomechanical changes in the TM tissue has been noticed with DEX treatment [195]. This appears that biomechanical alteration in POAG eyes may affect several locations to increase susceptibility to the damage of elevated IOP. However, the mechanisms of biomechanical changes of the tissue under chronically elevated IOP are not clear, nor are the properties of TM cells. Such investigations are currently underway with our collaborators.

Cultured CTM cells provide a useful platform for large scale *in vitro* compound screening to discover potential therapies for glaucoma and to understand their effects on molecular pathways. For example, a novel Rho kinase inhibitor, K-115, was found to disrupt actin bundles within the TM cells, thereby reducing their stiffness and resulting in decreased trabecular resistance [197]. Although most compounds are focused on reducing outflow resistance, measuring outflow resistance can be an issue *in vitro.* 3D-scaffod with seeded TM cells to simulate TM tissue *in vivo* are under development developing to overcome this difficulty [198]. This system could be applied to our CTM cells to screen potential drugs and study therapeutic effects. We also intent to perform other compound screenings in collaboration with the MSU Assay Development and Drug Repurposing Core.

Furthermore, CTM cells can be a used for *in vitro* screening of novel gene therapies. Modification of gene expression in the TM cells by gene therapy is one of the major approaches in the development of future, long-term IOP control [199,200]. For example, self-complementary adeno-associated virus (AAV) vectors containing the MMP1 (matrix metalloproteinase 1) cDNA have been successful delivered to the TM of the *in vivo* sheep model [201]. Non-viral vectors like small interfering RNAs to suppress *MYOC* expression in TM cells *in vitro* have been investigated [202]. Easy administration and sustained therapeutic effects makes it a potential target

for more effective treatment of glaucoma [203]. Moreover, several successful ocular AAV-mediated gene therapies have been or are in the process of being translated from dogs into clinical trials, such as for Leber congenital amaurosis [141] and achromatopsia [142]. This has emphasized the important role of canine disease models in gene therapy development. Therefore, we are interested in whether these CTM cells can be transfected by virus vectors, such as AAV, to select the optimal virus vectors for gene therapy in future.

Finally, CTM cells are not only suitable for compound screening and gene therapy development but can also be applied to gene editing with CRISPR-associated protein-9 nuclease (Cas9) [204]. Gene-modified TM cells can be transferred back to the TM tissue to replace the malfunctioning TM cells as part of cell-based therapy. Moreover, the possibility of developing cell therapy based on induced pluripotent stem cells (iPSCs) as potential treatment of POAG has been investigated [162]. iPSCs-derived TM cells have successfully rescued POAG phenotypes in the *MYOC* mutant mouse [205]. This has been a thriving area in recent years and may be a new approach for treating glaucoma in the future. However, whether such genome editing techniques or iPSCs- based cell therapy can be applied on our CTM cells and dog model remains unknown. We would like to further investigate its therapeutic potential on our CTM cell strains in the future.

REFERENCES

REFERENCES

1. Kwon YH, Fingert JH, Kuehn MH, Alward WL. Primary open-angle glaucoma. *N Engl J Med.* 2009;360(11):1113-1124.

2. Moorthy RS, Mermoud A, Baerveldt G, Minckler DS, Lee PP, Rao NA. Glaucoma associated with uveitis. *Surv Ophthalmol.* 1997;41(5):361-394.

3. Radcliffe NM, Finger PT. Eye cancer related glaucoma: current concepts. *Surv Ophthalmol.* 2009;54(1):47-73.

4. Sivaraman KR, Patel CG, Vajaranant TS, Aref AA. Secondary pigmentary glaucoma in patients with underlying primary pigment dispersion syndrome. *Clin Ophthalmol.* 2013;7:561-566.

5. Weinreb RN, Khaw PT. Primary open-angle glaucoma. *Lancet.* 2004;363(9422):1711-1720.

6. Sommer A, Tielsch JM, Katz J, et al. Relationship between intraocular pressure and primary open angle glaucoma among white and black Americans. The Baltimore Eye Survey. *Arch Ophthalmol.* 1991;109(8):1090-1095.

7. Mi XS, Yuan TF, So KF. The current research status of normal tension glaucoma. *Clin Interv Aging.* 2014;9:1563-1571.

8. Sawada A, Rivera JA, Takagi D, Nishida T, Yamamoto T. Progression to Legal Blindness in Patients With Normal Tension Glaucoma: Hospital-Based Study. *Invest Ophthalmol Vis Sci.* 2015;56(6):3635-3641.

9. Quigley HA, Broman AT. The number of people with glaucoma worldwide in 2010 and 2020. *The British journal of ophthalmology.* 2006;90(3):262-267.

10. Boland MV, Quigley HA. Risk factors and open-angle glaucoma: classification and application. *J Glaucoma.* 2007;16(4):406-418.

11. Caprioli J, Varma R. Intraocular pressure: modulation as treatment for glaucoma. *Am J Ophthalmol.* 2011;152(3):340-344.e342.

12. Grippo TM, Liu JH, Zebardast N, Arnold TB, Moore GH, Weinreb RN. Twenty-four-hour pattern of intraocular pressure in untreated patients with ocular hypertension. *Invest Ophthalmol Vis Sci.* 2013;54(1):512-517.

13. Quigley HA, Vitale S. Models of open-angle glaucoma prevalence and incidence in the United States. *Invest Ophthalmol Vis Sci.* 1997;38(1):83-91.

14. Liton PB, Challa P, Stinnett S, Luna C, Epstein DL, Gonzalez P. Cellular senescence in the glaucomatous outflow pathway. *Exp Gerontol.* 2005;40(8-9):745-748.

15. Burgoyne CF. A biomechanical paradigm for axonal insult within the optic nerve head in aging and glaucoma. *Exp Eye Res.* 2011;93(2):120-132.

16. Fleischman D, Berdahl JP, Zaydlarova J, Stinnett S, Fautsch MP, Allingham RR. Cerebrospinal fluid pressure decreases with older age. *PLoS One.* 2012;7(12):e52664.

17. Ren R, Jonas JB, Tian G, et al. Cerebrospinal fluid pressure in glaucoma: a prospective study. *Ophthalmology.* 2010;117(2):259-266.

18. Tielsch JM, Katz J, Sommer A, Quigley HA, Javitt JC. Family history and risk of primary open angle glaucoma. The Baltimore Eye Survey. *Arch Ophthalmol.* 1994;112(1):69-73.

19. Wolfs RC, Klaver CC, Ramrattan RS, van Duijn CM, Hofman A, de Jong PT. Genetic risk of primary open-angle glaucoma. Population-based familial aggregation study. *Arch Ophthalmol.* 1998;116(12):1640-1645.

20. Fan BJ, Wang DY, Lam DS, Pang CP. Gene mapping for primary open angle glaucoma. *Clin Biochem.* 2006;39(3):249-258.

21. Stone EM, Fingert JH, Alward WL, et al. Identification of a gene that causes primary open angle glaucoma. *Science.* 1997;275(5300):668-670.

22. Sheffield VC, Stone EM, Alward WL, et al. Genetic linkage of familial open angle glaucoma to chromosome 1q21-q31. *Nat Genet.* 1993;4(1):47-50.

23. Stoilov I, Akarsu AN, Sarfarazi M. Identification of three different truncating mutations in cytochrome P4501B1 (CYP1B1) as the principal cause of primary congenital glaucoma (Buphthalmos) in families linked to the GLC3A locus on chromosome 2p21. *Human molecular genetics.* 1997;6(4):641-647.

24. Monemi S, Spaeth G, DaSilva A, et al. Identification of a novel adult-onset primary open-angle glaucoma (POAG) gene on 5q22.1. *Human molecular genetics.* 2005;14(6):725-733.

25. Sahlender DA, Roberts RC, Arden SD, et al. Optineurin links myosin VI to the Golgi complex and is involved in Golgi organization and exocytosis. *J Cell Biol.* 2005;169(2):285-295.

26. Rezaie T, Child A, Hitchings R, et al. Adult-onset primary open-angle glaucoma caused by mutations in optineurin. *Science.* 2002;295(5557):1077-1079.

27. Vollrath D, Jaramillo-Babb VL, Clough MV, et al. Loss-of-function mutations in the LIM-homeodomain gene, LMX1B, in nail-patella syndrome. *Hum Mol Genet.* 1998;7(7):1091-1098.

28. Lambert W, Agarwal R, Howe W, Clark AF, Wordinger RJ. Neurotrophin and neurotrophin receptor expression by cells of the human lamina cribrosa. *Invest Ophthalmol Vis Sci.* 2001;42(10):2315-2323.

29. Wirtz MK, Samples JR, Rust K, et al. GLC1F, a new primary open-angle glaucoma locus, maps to 7q35-q36. *Arch Ophthalmol.* 1999;117(2):237-241.

30. Pasutto F, Keller KE, Weisschuh N, et al. Variants in ASB10 are associated with open-angle glaucoma. *Hum Mol Genet.* 2012;21(6):1336-1349.

31. Klein BE, Klein R, Lee KE. Heritability of risk factors for primary open-angle glaucoma: the Beaver Dam Eye Study. *Invest Ophthalmol Vis Sci.* 2004;45(1):59-62.

32. Young TL, Metlapally R, Shay AE. Complex trait genetics of refractive error. *Arch Ophthalmol.* 2007;125(1):38-48.

33. Vincent AL, Billingsley G, Buys Y, et al. Digenic inheritance of early-onset glaucoma: CYP1B1, a potential modifier gene. *Am J Hum Genet.* 2002;70(2):448-460.

34. Footz T, Dubois S, Sarfarazi M, Raymond V, Walter MA. Co-variation of STI1 and WDR36/UTP21 alters cell proliferation in a glaucoma model. *Mol Vis.* 2011;17:1957-1969.

35. Footz TK, Johnson JL, Dubois S, Boivin N, Raymond V, Walter MA. Glaucoma-associated WDR36 variants encode functional defects in a yeast model system. *Hum Mol Genet.* 2009;18(7):1276-1287.

36. De Marco N, Buono M, Troise F, Diez-Roux G. Optineurin increases cell survival and translocates to the nucleus in a Rab8-dependent manner upon an apoptotic stimulus. *J Biol Chem.* 2006;281(23):16147-16156.

37. Morello R, Zhou G, Dreyer SD, et al. Regulation of glomerular basement membrane collagen expression by LMX1B contributes to renal disease in nail patella syndrome. *Nat Genet.* 2001;27(2):205-208.

38. Riddle RD, Ensini M, Nelson C, Tsuchida T, Jessell TM, Tabin C. Induction of the LIM homeobox gene Lmx1 by WNT7a establishes dorsoventral pattern in the vertebrate limb. *Cell.* 1995;83(4):631-640.

39. Vogel A, Rodriguez C, Warnken W, Izpisúa Belmonte JC. Dorsal cell fate specified by chick Lmx1 during vertebrate limb development. *Nature.* 1995;378(6558):716-720.

40. Pasutto F, Matsumoto T, Mardin CY, et al. Heterozygous NTF4 mutations impairing neurotrophin-4 signaling in patients with primary open-angle glaucoma. *American journal of human genetics.* 2009;85(4):447-456.

41. Pease ME, McKinnon SJ, Quigley HA, Kerrigan-Baumrind LA, Zack DJ. Obstructed axonal transport of BDNF and its receptor TrkB in experimental glaucoma. *Invest Ophthalmol Vis Sci.* 2000;41(3):764-774.

42. Racette L, Wilson MR, Zangwill LM, Weinreb RN, Sample PA. Primary open-angle glaucoma in blacks: a review. *Surv Ophthalmol.* 2003;48(3):295-313.

43. Ashaye A, Ashaolu O, Komolafe O, et al. Prevalence and types of glaucoma among an indigenous African population in southwestern Nigeria. *Invest Ophthalmol Vis Sci.* 2013;54(12):7410-7416.

44. Cook C. Glaucoma in Africa: size of the problem and possible solutions. *J Glaucoma.* 2009;18(2):124-128.

45. Rotchford AP, Johnson GJ. Glaucoma in Zulus: a population-based cross-sectional survey in a rural district in South Africa. *Arch Ophthalmol.* 2002;120(4):471-478.

46. To CH, Kong CW, Chan CY, Shahidullah M, Do CW. The mechanism of aqueous humour formation. *Clin Exp Optom.* 2002;85(6):335-349.

47. Goel M, Picciani RG, Lee RK, Bhattacharya SK. Aqueous humor dynamics: a review. *Open Ophthalmol J.* 2010;4:52-59.

48. Gabelt BT, Kaufman PL. Changes in aqueous humor dynamics with age and glaucoma. *Prog Retin Eye Res.* 2005;24(5):612-637.

49. Dunn JJ, Lytle C, Crook RB. Immunolocalization of the Na-K-Cl cotransporter in bovine ciliary epithelium. *Invest Ophthalmol Vis Sci.* 2001;42(2):343-353.

50. Delamere NA. Ciliary Body and Ciliary Epithelium. *Adv Organ Biol.* 2005;10:127-148.

51. Mark HH. Aqueous humor dynamics in historical perspective. *Surv Ophthalmol.* 2010;55(1):89-100.

52. Pizzirani S, Gong H. Functional Anatomy of the Outflow Facilities. *Vet Clin North Am Small Anim Pract.* 2015;45(6):1101-1126, v.

53. To CH, Do CW, Zamudio AC, Candia OA. Model of ionic transport for bovine ciliary epithelium: effects of acetazolamide and HCO. *Am J Physiol Cell Physiol.* 2001;280(6):C1521-1530.

54. Stamer WD, Acott TS. Current understanding of conventional outflow dysfunction in glaucoma. *Current opinion in ophthalmology.* 2012;23(2):135-143.

55. Nilsson SF. The uveoscleral outflow routes. *Eye (Lond).* 1997;11 (Pt 2):149-154.

56. FLOCKS M. The anatomy of the trabecular meshwork as seen in tangential section. *AMA Arch Ophthalmol.* 1956;56(5):708-718.

57. Tektas OY, Lutjen-Drecoll E. Structural changes of the trabecular meshwork in different kinds of glaucoma. *Experimental eye research.* 2009;88(4):769-775.

58. Gong H, Tripathi RC, Tripathi BJ. Morphology of the aqueous outflow pathway. *Microsc Res Tech.* 1996;33(4):336-367.

59. Lei Y, Overby DR, Boussommier-Calleja A, Stamer WD, Ethier CR. Outflow physiology of the mouse eye: pressure dependence and washout. *Invest Ophthalmol Vis Sci.* 2011;52(3):1865-1871.

60. Smit BA, Johnstone MA. Effects of viscoelastic injection into Schlemm's canal in primate and human eyes: potential relevance to viscocanalostomy. *Ophthalmology.* 2002;109(4):786-792.

61. Samuelson, DA, Gelatt, KN. Aqueous outflow in the beagle. II. Postnatal morphologic development of the iridocorneal angle: corneoscleral trabecular meshwork and angular aqueous plexus. *Curr Eye Res.*1984;3(6):795-807.

62. McLellan GJ, Miller PE. Feline glaucoma--a comprehensive review. *Vet Ophthalmol.* 2011;14 Suppl 1:15-29.

63. McMenamin PG, Steptoe RJ. Normal anatomy of the aqueous humour outflow system in the domestic pig eye. *J Anat.* 1991;178:65-77.

64. Samuelson D, Smith P, Brooks D. Morphologic features of the aqueous humor drainage pathways in horses. *Am J Vet Res.* 1989;50(5):720-727.

65. Edward DP, Bouhenni R. Anterior segment alterations and comparative aqueous humor proteomics in the buphthalmic rabbit (an American Ophthalmological Society thesis). *Trans Am Ophthalmol Soc.* 2011;109:66-114.

66. Gray MP, Smith RS, Soules KA, John SW, Link BA. The aqueous humor outflow pathway of zebrafish. *Invest Ophthalmol Vis Sci.* 2009;50(4):1515-1521.

67. Gould DB, Smith RS, John SW. Anterior segment development relevant to glaucoma. *Int J Dev Biol.* 2004;48(8-9):1015-1029.

68. Kelley MJ, Rose AY, Keller KE, Hessle H, Samples JR, Acott TS. Stem cells in the trabecular meshwork: present and future promises. *Exp Eye Res.* 2009;88(4):747-751.

69. Tamm ER. The trabecular meshwork outflow pathways: structural and functional aspects. *Experimental eye research.* 2009;88(4):648-655.

70. Lütjen-Drecoll E. Functional morphology of the trabecular meshwork in primate eyes. *Prog Retin Eye Res.* 1999;18(1):91-119.

71. Marshall GE, Konstas AG, Lee WR. Immunogold localization of type IV collagen and laminin in the aging human outflow system. *Exp Eye Res.* 1990;51(6):691-699.

72. Johnson M. 'What controls aqueous humour outflow resistance?'. *Experimental eye research.* 2006;82(4):545-557.

73. Hann CR, Fautsch MP. Preferential fluid flow in the human trabecular meshwork near collector channels. *Invest Ophthalmol Vis Sci.* 2009;50(4):1692-1697.

74. Stamer DW, Roberts BC, Epstein DL, Allingham RR. Isolation of primary open-angle glaucomatous trabecular meshwork cells from whole eye tissue. *Curr Eye Res.* 2000;20(5):347-350.

75. Hoare MJ, Grierson I, Brotchie D, Pollock N, Cracknell K, Clark AF. Cross-linked actin networks (CLANs) in the trabecular meshwork of the normal and glaucomatous human eye in situ. *Investigative ophthalmology & visual science.* 2009;50(3):1255-1263.

76. Kuchtey J, Kuchtey RW. The microfibril hypothesis of glaucoma: implications for treatment of elevated intraocular pressure. *Journal of ocular pharmacology and therapeutics : the official journal of the Association for Ocular Pharmacology and Therapeutics.* 2014;30(2-3):170-180.

77. Vranka JA, Kelley MJ, Acott TS, Keller KE. Extracellular matrix in the trabecular meshwork: intraocular pressure regulation and dysregulation in glaucoma. *Exp Eye Res.* 2015;133:112-125.

78. Tripathi RC, Li J, Chan WF, Tripathi BJ. Aqueous humor in glaucomatous eyes contains an increased level of TGF-beta 2. *Experimental eye research.* 1994;59(6):723-727.

79. Penn JW, Grobbelaar AO, Rolfe KJ. The role of the TGF-β family in wound healing, burns and scarring: a review. *Int J Burns Trauma.* 2012;2(1):18-28.

80. Fleenor DL, Shepard AR, Hellberg PE, Jacobson N, Pang IH, Clark AF. TGFbeta2-induced changes in human trabecular meshwork: implications for intraocular pressure. *Investigative ophthalmology & visual science.* 2006;47(1):226-234.

81. Howell KG, Vrabel AM, Chowdhury UR, Stamer WD, Fautsch MP. Myocilin levels in primary open-angle glaucoma and pseudoexfoliation glaucoma human aqueous humor. *Journal of glaucoma.* 2010;19(9):569-575.

82. Kroeber M, Davis N, Holzmann S, et al. Reduced expression of Pax6 in lens and cornea of mutant mice leads to failure of chamber angle development and juvenile glaucoma. *Hum Mol Genet.* 2010;19(17):3332-3342.

83. Ali M, McKibbin M, Booth A, et al. Null mutations in LTBP2 cause primary congenital glaucoma. *American journal of human genetics.* 2009;84(5):664-671.

84. Lim SH, Tran-Viet KN, Yanovitch TL, et al. CYP1B1, MYOC, and LTBP2 mutations in primary congenital glaucoma patients in the United States. *American journal of ophthalmology.* 2013;155(3):508-517 e505.

85. Chen Y, Jiang D, Yu L, et al. CYP1B1 and MYOC mutations in 116 Chinese patients with primary congenital glaucoma. *Arch Ophthalmol.* 2008;126(10):1443-1447.

86. Huang W, Jaroszewski J, Ortego J, Escribano J, Coca-Prados M. Expression of the TIGR gene in the iris, ciliary body, and trabecular meshwork of the human eye. *Ophthalmic Genet.* 2000;21(3):155-169.

87. Tamm ER. Myocilin and glaucoma: facts and ideas. *Prog Retin Eye Res.* 2002;21(4):395-428.

88. Jacobson N, Andrews M, Shepard AR, et al. Non-secretion of mutant proteins of the glaucoma gene myocilin in cultured trabecular meshwork cells and in aqueous humor. *Hum Mol Genet.* 2001;10(2):117-125.

89. Sall K. The efficacy and safety of brinzolamide 1% ophthalmic suspension (Azopt) as a primary therapy in patients with open-angle glaucoma or ocular hypertension. Brinzolamide Primary Therapy Study Group. *Surv Ophthalmol.* 2000;44 Suppl 2:S155-162.

90. van der Valk R, Webers CA, Schouten JS, Zeegers MP, Hendrikse F, Prins MH. Intraocular pressure-lowering effects of all commonly used glaucoma drugs: a meta-analysis of randomized clinical trials. *Ophthalmology.* 2005;112(7):1177-1185.

91. Challa P, Arnold JJ. Rho-kinase inhibitors offer a new approach in the treatment of glaucoma. *Expert Opin Investig Drugs.* 2014;23(1):81-95.

92. Kaplowitz K, Kuei A, Klenofsky B, Abazari A, Honkanen R. The use of endoscopic cyclophotocoagulation for moderate to advanced glaucoma. *Acta Ophthalmol.* 2015;93(5):395-401.

93. Nordmann JP, Mertz B, Yannoulis NC, et al. A double-masked randomized comparison of the efficacy and safety of unoprostone with timolol and betaxolol in patients with

primary open-angle glaucoma including pseudoexfoliation glaucoma or ocular hypertension. 6 month data. *Am J Ophthalmol.* 2002;133(1):1-10.

94. Orzalesi N, Rossetti L, Bottoli A, Fumagalli E, Fogagnolo P. The effect of latanoprost, brimonidine, and a fixed combination of timolol and dorzolamide on circadian intraocular pressure in patients with glaucoma or ocular hypertension. *Arch Ophthalmol.* 2003;121(4):453-457.

95. Stewart RH, Kimbrough RL, Ward RL. Betaxolol vs timolol. A six-month double-blind comparison. *Arch Ophthalmol.* 1986;104(1):46-48.

96. Stewart WC, Laibovitz R, Horwitz B, Stewart RH, Ritch R, Kottler M. A 90-day study of the efficacy and side effects of 0.25% and 0.5% apraclonidine vs 0.5% timolol. Apraclonidine Primary Therapy Study Group. *Arch Ophthalmol.* 1996;114(8):938-942.

97. Katz LJ. Brimonidine tartrate 0.2% twice daily vs timolol 0.5% twice daily: 1-year results in glaucoma patients. Brimonidine Study Group. *Am J Ophthalmol.* 1999;127(1):20-26.

98. Liu JH, Medeiros FA, Slight JR, Weinreb RN. Diurnal and nocturnal effects of brimonidine monotherapy on intraocular pressure. *Ophthalmology.* 2010;117(11):2075-2079.

99. Toris CB, Camras CB, Yablonski ME. Acute versus chronic effects of brimonidine on aqueous humor dynamics in ocular hypertensive patients. *Am J Ophthalmol.* 1999;128(1):8-14.

100. Brinchmann-Hansen O, Albrektsen T, Anmarkrud N. Pilocarpine drops do not reduce intraocular pressure sufficiently in pseudoexfoliation glaucoma. *Eye (Lond).* 1993;7 (Pt 4):511-516.

101. Reichert RW, Shields MB. Intraocular pressure response to the replacement of pilocarpine or carbachol with echothiophate. *Graefes Arch Clin Exp Ophthalmol.* 1991;229(3):252-253.

102. Tanihara H, Inoue T, Yamamoto T, et al. Phase 1 clinical trials of a selective Rho kinase inhibitor, K-115. *JAMA Ophthalmol.* 2013;131(10):1288-1295.

103. Waki M, Yoshida Y, Oka T, Azuma M. Reduction of intraocular pressure by topical administration of an inhibitor of the Rho-associated protein kinase. *Curr Eye Res.* 2001;22(6):470-474.

104. Awasthi P, Srivastava SN. Role of oral glycerol in glaucoma. *Br J Ophthalmol.* 1965;49(12):660-666.

105. Volopich S, Mosing M, Auer U, Nell B. Comparison of the effect of hypertonic hydroxyethyl starch and mannitol on the intraocular pressure in healthy normotensive

dogs and the effect of hypertonic hydroxyethyl starch on the intraocular pressure in dogs with primary glaucoma. *Vet Ophthalmol.* 2006;9(4):239-244.

106. Martínez A, Sánchez M. Effects of dorzolamide 2% added to timolol maleate 0.5% on intraocular pressure, retrobulbar blood flow, and the progression of visual field damage in patients with primary open-angle glaucoma: a single-center, 4-year, open-label study. *Clin Ther.* 2008;30(6):1120-1134.

107. Oztürk F, Ermiş SS, Inan UU, Aşagidag A, Yaman S. Comparison of the efficacy and safety of dorzolamide 2% when added to brimonidine 0.2% or timolol maleate 0.5% in patients with primary open-angle glaucoma. *J Ocul Pharmacol Ther.* 2005;21(1):68-74.

108. Hamacher T, Schinzel M, Schölzel-Klatt A, et al. Short term efficacy and safety in glaucoma patients changed to the latanoprost 0.005%/timolol maleate 0.5% fixed combination from monotherapies and adjunctive therapies. *Br J Ophthalmol.* 2004;88(10):1295-1298.

109. Greig SL, Deeks ED. Brinzolamide/brimonidine: a review of its use in patients with open-angle glaucoma or ocular hypertension. *Drugs Aging.* 2015;32(3):251-260.

110. Schnober D, Hubatsch DA, Scherzer ML. Efficacy and safety of fixed-combination travoprost 0.004%/timolol 0.5% in patients transitioning from bimatoprost 0.03%/timolol 0.5% combination therapy. *Clin Ophthalmol.* 2015;9:825-832.

111. Murthy GJ, Murthy PR, Murthy KR, Kulkarni VV. A study of the efficacy of endoscopic cyclophotocoagulation for the treatment of refractory glaucomas. *Indian J Ophthalmol.* 2009;57(2):127-132.

112. Lindfield D, Ritchie RW, Griffiths MF. 'Phaco-ECP': combined endoscopic cyclophotocoagulation and cataract surgery to augment medical control of glaucoma. *BMJ Open.* 2012;2(3).

113. The Glaucoma Laser Trial (GLT). 2. Results of argon laser trabeculoplasty versus topical medicines. The Glaucoma Laser Trial Research Group. *Ophthalmology.* 1990;97(11):1403-1413.

114. Rafuse PE. The optimal trabeculectomy: patient and procedure. *Can J Ophthalmol.* 2014;49(6):523-527.

115. Gedde SJ, Schiffman JC, Feuer WJ, et al. Treatment outcomes in the Tube Versus Trabeculectomy (TVT) study after five years of follow-up. *Am J Ophthalmol.* 2012;153(5):789-803.e782.

116. Morrison JC, Moore CG, Deppmeier LM, Gold BG, Meshul CK, Johnson EC. A rat model of chronic pressure-induced optic nerve damage. *Exp Eye Res.* 1997;64(1):85-96.

117. Dawson WW, Brooks DE, Hope GM, et al. Primary open angle glaucomas in the rhesus monkey. *Br J Ophthalmol.* 1993;77(5):302-310.

118. Gaasterland D, Kupfer C. Experimental glaucoma in the rhesus monkey. *Invest Ophthalmol.* 1974;13(6):455-457.

119. Weber AJ, Zelenak D. Experimental glaucoma in the primate induced by latex microspheres. *J Neurosci Methods.* 2001;111(1):39-48.

120. Kuchtey J, Olson LM, Rinkoski T, et al. Mapping of the disease locus and identification of ADAMTS10 as a candidate gene in a canine model of primary open angle glaucoma. *PLoS Genet.* 2011;7(2):e1001306.

121. Kuchtey J, Kunkel J, Esson D, et al. Screening ADAMTS10 in dog populations supports Gly661Arg as the glaucoma-causing variant in beagles. *Investigative ophthalmology & visual science.* 2013;54(3):1881-1886.

122. Teixeira LB, Buhr KA, Bowie O, et al. Quantifying optic nerve axons in a cat glaucoma model by a semi-automated targeted counting method. *Molecular vision.* 2014;20:376-385.

123. Kuehn MH, Lipsett KA, Menotti-Raymond M, et al. A Mutation in LTBP2 Causes Congenital Glaucoma in Domestic Cats (Felis catus). *PLoS One.* 2016;11(5):e0154412.

124. Gerometta R, Podos SM, Danias J, Candia OA. Steroid-induced ocular hypertension in normal sheep. *Investigative ophthalmology & visual science.* 2009;50(2):669-673.

125. Gerometta R, Podos SM, Candia OA, et al. Steroid-induced ocular hypertension in normal cattle. *Arch Ophthalmol.* 2004;122(10):1492-1497.

126. Ticho U, Lahav M, Berkowitz S, Yoffe P. Ocular changes in rabbits with corticosteroid-induced ocular hypertension. *Br J Ophthalmol.* 1979;63(9):646-650.

127. Zhou Y, Grinchuk O, Tomarev SI. Transgenic mice expressing the Tyr437His mutant of human myocilin protein develop glaucoma. *Invest Ophthalmol Vis Sci.* 2008;49(5):1932-1939.

128. Chi ZL, Akahori M, Obazawa M, et al. Overexpression of optineurin E50K disrupts Rab8 interaction and leads to a progressive retinal degeneration in mice. *Hum Mol Genet.* 2010;19(13):2606-2615.

129. Dai Y, Lindsey JD, Duong-Polk X, Nguyen D, Hofer A, Weinreb RN. Outflow facility in mice with a targeted type I collagen mutation. *Invest Ophthalmol Vis Sci.* 2009;50(12):5749-5753.

130. Veth KN, Willer JR, Collery RF, et al. Mutations in zebrafish lrp2 result in adult-onset ocular pathogenesis that models myopia and other risk factors for glaucoma. *PLoS Genet.* 2011;7(2):e1001310.

131. Hann CR, Vercnocke AJ, Bentley MD, Jorgensen SM, Fautsch MP. Anatomic changes in Schlemm's canal and collector channels in normal and primary open-angle glaucoma eyes using low and high perfusion pressures. *Invest Ophthalmol Vis Sci.* 2014;55(9):5834-5841.

132. Mao W, Tovar-Vidales T, Yorio T, Wordinger RJ, Clark AF. Perfusion-cultured bovine anterior segments as an ex vivo model for studying glucocorticoid-induced ocular hypertension and glaucoma. *Investigative ophthalmology & visual science.* 2011;52(11):8068-8075.

133. Gelatt KN, MacKay EO. Prevalence of the breed-related glaucomas in pure-bred dogs in North America. *Veterinary ophthalmology.* 2004;7(2):97-111.

134. Gelatt KN, Peiffer RL, Gwin RM, Gum GG, Williams LW. Clinical manifestations of inherited glaucoma in the beagle. *Invest Ophthalmol Vis Sci.* 1977;16(12):1135-1142.

135. Brooks DE, Strubbe DT, Kubilis PS, MacKay EO, Samuelson DA, Gelatt KN. Histomorphometry of the optic nerves of normal dogs and dogs with hereditary glaucoma. *Experimental eye research.* 1995;60(1):71-89.

136. Gelatt KN, Mackay EO. The ocular hypertensive effects of topical 0.1% dexamethasone in beagles with inherited glaucoma. *J Ocul Pharmacol Ther.* 1998;14(1):57-66.

137. Samuelson DA, Gum GG, Gelatt KN. Ultrastructural changes in the aqueous outflow apparatus of beagles with inherited glaucoma. *Investigative ophthalmology & visual science.* 1989;30(3):550-561.

138. Mackay EO, McLaughlin M, Plummer CE, Ben-Shlomo A, Gelatt KN. Dose response for travoprost® in the glaucomatous beagle. *Vet Ophthalmol.* 2012;15 Suppl 1:31-35.

139. Gelatt KN, Gum GG, Brooks DE, Wolf ED, Bromberg NM. Dose response of topical pilocarpine-epinephrine combinations in normotensive and glaucomatous Beagles. *Am J Vet Res.* 1983;44(11):2018-2027.

140. Gelatt KN, MacKay EO. Effect of different dose schedules of latanoprost on intraocular pressure and pupil size in the glaucomatous Beagle. *Veterinary ophthalmology.* 2001;4(4):283-288.

141. Cideciyan AV, Jacobson SG, Beltran WA, et al. Human retinal gene therapy for Leber congenital amaurosis shows advancing retinal degeneration despite enduring visual improvement. *Proceedings of the National Academy of Sciences of the United States of America.* 2013;110(6):E517-525.

142. Komaromy AM, Rowlan JS, Corr AT, et al. Transient photoreceptor deconstruction by CNTF enhances rAAV-mediated cone functional rescue in late stage CNGB3-achromatopsia. *Molecular therapy : the journal of the American Society of Gene Therapy.* 2013;21(6):1131-1141.

143. Wade NC, Grierson I, O'Reilly S, et al. Cross-linked actin networks (CLANs) in bovine trabecular meshwork cells. *Experimental eye research.* 2009;89(5):648-659.

144. Mao W, Liu Y, Mody A, Montecchi-Palmer M, Wordinger RJ, Clark AF. Characterization of a spontaneously immortalized bovine trabecular meshwork cell line. *Experimental eye research.* 2012;105:53-59.

145. Clark AF, Wilson K, McCartney MD, Miggans ST, Kunkle M, Howe W. Glucocorticoid-induced formation of cross-linked actin networks in cultured human trabecular meshwork cells. *Investigative ophthalmology & visual science.* 1994;35(1):281-294.

146. Clark AF, Steely HT, Dickerson JE, et al. Glucocorticoid induction of the glaucoma gene MYOC in human and monkey trabecular meshwork cells and tissues. *Invest Ophthalmol Vis Sci.* 2001;42(8):1769-1780.

147. Mao W, Liu Y, Wordinger RJ, Clark AF. A magnetic bead-based method for mouse trabecular meshwork cell isolation. *Invest Ophthalmol Vis Sci.* 2013;54(5):3600-3606.

148. Kim GA, Oh HJ, Kim MJ, et al. Effect of primary culture medium type for culture of canine fibroblasts on production of cloned dogs. *Theriogenology.* 2015;84(4): 524-30.

149. Vangipuram M, Ting D, Kim S, Diaz R, Schüle B. Skin punch biopsy explant culture for derivation of primary human fibroblasts. *J Vis Exp.* 2013(77):e3779.

150. Lin S, Lee OT, Minasi P, Wong J. Isolation, culture, and characterization of human fetal trabecular meshwork cells. *Curr Eye Res.* 2007;32(1):43-50.

151. Morgan JT, Wood JA, Walker NJ, et al. Human trabecular meshwork cells exhibit several characteristics of, but are distinct from, adipose-derived mesenchymal stem cells. *Journal of ocular pharmacology and therapeutics : the official journal of the Association for Ocular Pharmacology and Therapeutics.* 2014;30(2-3):254-266.

152. Polansky JR, Fauss DJ, Zimmerman CC. Regulation of TIGR/MYOC gene expression in human trabecular meshwork cells. *Eye (Lond).* 2000;14 (Pt 3B):503-514.

153. Porter KM, Epstein DL, Liton PB. Up-regulated expression of extracellular matrix remodeling genes in phagocytically challenged trabecular meshwork cells. *PLoS One.* 2012;7(4):e34792.

154. Comes N, Buie LK, Borras T. Evidence for a role of angiopoietin-like 7 (ANGPTL7) in extracellular matrix formation of the human trabecular meshwork: implications for glaucoma. *Genes Cells.* 2011;16(2):243-259.

155. Liton PB, Luna C, Challa P, Epstein DL, Gonzalez P. Genome-wide expression profile of human trabecular meshwork cultured cells, nonglaucomatous and primary open angle glaucoma tissue. *Mol Vis.* 2006;12:774-790.

156. Stamer WD, Seftor RE, Snyder RW, Regan JW. Cultured human trabecular meshwork cells express aquaporin-1 water channels. *Curr Eye Res.* 1995;14(12):1095-1100.

157. Yue BY, Kurosawa A, Elvart JL, Elner VM, Tso MO. Monkey trabecular meshwork cells in culture: growth, morphologic, and biochemical characteristics. *Graefes Arch Clin Exp Ophthalmol.* 1988;226(3):262-268.

158. Chang IL, Elner G, Yue YJ, Cornicelli A, Kawa JE, Elner VM. Expression of modified low-density lipoprotein receptors by trabecular meshwork cells. *Curr Eye Res.* 1991;10(12):1101-1112.

159. Pfeffer BA, DeWitt CA, Salvador-Silva M, Cavet ME, López FJ, Ward KW. Reduced myocilin expression in cultured monkey trabecular meshwork cells induced by a selective glucocorticoid receptor agonist: comparison with steroids. *Invest Ophthalmol Vis Sci.* 2010;51(1):437-446.

160. Li J, Tripathi BJ, Tripathi RC. Modulation of pre-mRNA splicing and protein production of fibronectin by TGF-beta2 in porcine trabecular cells. *Invest Ophthalmol Vis Sci.* 2000;41(11):3437-3443.

161. Begley CG, Yue BY, Hendricks RL. Murine trabecular meshwork cells in tissue culture. *Curr Eye Res.* 1991;10(11):1015-1030.

162. Ding QJ, Zhu W, Cook AC, Anfinson KR, Tucker BA, Kuehn MH. Induction of trabecular meshwork cells from induced pluripotent stem cells. *Investigative ophthalmology & visual science.* 2014;55(11):7065-7072.

163. O'Reilly S, Pollock N, Currie L, Paraoan L, Clark AF, Grierson I. Inducers of cross-linked actin networks in trabecular meshwork cells. *Investigative ophthalmology & visual science.* 2011;52(10):7316-7324.

164. Clark AF, Brotchie D, Read AT, et al. Dexamethasone alters F-actin architecture and promotes cross-linked actin network formation in human trabecular meshwork tissue. *Cell Motil Cytoskeleton.* 2005;60(2):83-95.

165. Hart H, Samuelson DA, Tajwar H, et al. Immunolocalization of myocilin protein in the anterior eye of normal and primary open-angle glaucomatous dogs. *Vet Ophthalmol.* 2007;10 Suppl 1:28-37.

166. Livak KJ, Schmittgen TD. Analysis of relative gene expression data using real-time quantitative PCR and the 2(-Delta Delta C(T)) Method. *Methods.* 2001;25(4):402-408.

167. Tamm ER, Russell P, Piatigorsky J. Development of characterization of a immortal and differentiated murine trabecular meshwork cell line. *Investigative ophthalmology & visual science.* 1999;40(7):1392-1403.

168. Fautsch MP, Howell KG, Vrabel AM, Charlesworth MC, Muddiman DC, Johnson DH. Primary trabecular meshwork cells incubated in human aqueous humor differ from cells incubated in serum supplements. *Invest Ophthalmol Vis Sci.* 2005;46(8):2848-2856.

169. Yamazaki Y, Matsunaga H, Nishikawa M, et al. Senescence in cultured trabecular meshwork cells. *Br J Ophthalmol.* 2007;91(6):808-811.

170. Pang IH, Shade DL, Clark AF, Steely HT, DeSantis L. Preliminary characterization of a transformed cell strain derived from human trabecular meshwork. *Current eye research.* 1994;13(1):51-63.

171. Hassel B, Samuelson DA, Lewis PA, Gelatt KN. Immunocytochemical localization of smooth muscle actin-containing cells in the trabecular meshwork of glaucomatous and nonglaucomatous dogs. *Veterinary ophthalmology.* 2007;10 Suppl 1:38-45.

172. Buller C, Johnson DH, Tschumper RC. Human trabecular meshwork phagocytosis. Observations in an organ culture system. *Invest Ophthalmol Vis Sci.* 1990;31(10):2156-2163.

173. Zhang X, Ognibene CM, Clark AF, Yorio T. Dexamethasone inhibition of trabecular meshwork cell phagocytosis and its modulation by glucocorticoid receptor beta. *Exp Eye Res.* 2007;84(2):275-284.

174. Johnson DH, Richardson TM, Epstein DL. Trabecular meshwork recovery after phagocytic challenge. *Curr Eye Res.* 1989;8(11):1121-1130.

175. Currie LM, Job R, Paraoan L, Grierson I. Do Cross-linked Actin Networks Form In Cells Other Than The Trabecular Meshwork? 2011;52(14):4665-4665.

176. McIntire DJ. Conjunctival incision and trabeculectomy. *Ophthalmic Surg.* 1977;8(2):139.

177. Phillips CI. Trabeculectomy without conjunctival incision. *Am J Ophthalmol.* 1992;114(1):108-109.

178. Dawson-Baglien EM, Winkler PA, Bruewer AR, Petersen-Jones SM, Bartoe JT. Isolation and cultivation of canine uveal melanocytes. *Veterinary ophthalmology.* 2015;18(4):285-290.

179. Job R, Raja V, Grierson I, et al. Cross-linked actin networks (CLANs) are present in lamina cribrosa cells. *Br J Ophthalmol.* 2010;94(10):1388-1392.

180. Wu Y, Chen W, Guo M, He Q, Hu Y. Effects of transforming growth factor-β2 on myocilin expression and secretion in human primary cultured trabecular meshwork cells. *Int J Clin Exp Pathol.* 2014;7(8):4827-4836.

181. Lo WR, Rowlette LL, Caballero M, Yang P, Hernandez MR, Borrás T. Tissue differential microarray analysis of dexamethasone induction reveals potential mechanisms of steroid glaucoma. *Invest Ophthalmol Vis Sci.* 2003;44(2):473-485.

182. Ishibashi T, Takagi Y, Mori K, et al. cDNA microarray analysis of gene expression changes induced by dexamethasone in cultured human trabecular meshwork cells. *Invest Ophthalmol Vis Sci.* 2002;43(12):3691-3697.

183. Leung YF, Tam PO, Lee WS, et al. The dual role of dexamethasone on anti-inflammation and outflow resistance demonstrated in cultured human trabecular meshwork cells. *Mol Vis.* 2003;9:425-439.

184. Rozsa FW, Reed DM, Scott KM, et al. Gene expression profile of human trabecular meshwork cells in response to long-term dexamethasone exposure. *Mol Vis.* 2006;12:125-141.

185. Overby DR, Bertrand J, Tektas OY, et al. Ultrastructural changes associated with dexamethasone-induced ocular hypertension in mice. *Invest Ophthalmol Vis Sci.* 2014;55(8):4922-4933.

186. Driscoll A, Blizzard C. Toxicity and Pharmacokinetics of Sustained-Release Dexamethasone in Beagle Dogs. *Adv Ther.* 2016;33(1):58-67.

187. Karamichos D, Lakshman N, Petroll WM. Regulation of corneal fibroblast morphology and collagen reorganization by extracellular matrix mechanical properties. *Invest Ophthalmol Vis Sci.* 2007;48(11):5030-5037.

188. Harrison SA, Mondino BJ, Mayer FJ. Scleral fibroblasts. Human leukocyte antigen expression and complement production. *Invest Ophthalmol Vis Sci.* 1990;31(11):2412-2419.

189. Welge-Lüssen U, Eichhorn M, Bloemendal H, Lütjen-Drecoll E. Classification of human scleral spur cells in monolayer culture. *Eur J Cell Biol.* 1998;75(1):78-84.

190. Tamm E, Flügel C, Baur A, Lütjen-Drecoll E. Cell cultures of human ciliary muscle: growth, ultrastructural and immunocytochemical characteristics. *Exp Eye Res.* 1991;53(3):375-387.

191. Caprioli J. Glaucoma: a disease of early cellular senescence. *Invest Ophthalmol Vis Sci.* 2013;54(14):ORSF60-67.

192. Pleyer U, Ursell PG, Rama P. Intraocular pressure effects of common topical steroids for post-cataract inflammation: are they all the same? *Ophthalmol Ther.* 2013;2(2):55-72.

193. Tektas OY, Lütjen-Drecoll E. Structural changes of the trabecular meshwork in different kinds of glaucoma. *Exp Eye Res.* 2009;88(4):769-775.

194. Morales J, Al-Sharif L, Khalil DS, et al. Homozygous mutations in ADAMTS10 and ADAMTS17 cause lenticular myopia, ectopia lentis, glaucoma, spherophakia, and short stature. *Am J Hum Genet.* 2009;85(5):558-568.

195. Raghunathan VK, Morgan JT, Park SA, et al. Dexamethasone Stiffens Trabecular Meshwork, Trabecular Meshwork Cells, and Matrix. *Invest Ophthalmol Vis Sci.* 2015;56(8):4447-4459.

196. Boote C, Palko JR, Sorensen T, et al. Changes in posterior scleral collagen microstructure in canine eyes with an ADAMTS10 mutation. *Molecular vision.* 2016;22:503-517.

197. Kaneko Y, Ohta M, Inoue T, et al. Effects of K-115 (Ripasudil), a novel ROCK inhibitor, on trabecular meshwork and Schlemm's canal endothelial cells. *Sci Rep.* 2016;6:19640.

198. Bernier S, Krebs M, Pantcheva MB. 3D Natural Biopolymer Scaffold for In Vitro Modeling of the Trabecular Meshwork. *Investigative Ophthalmology & Visual Science.* 2015;56(7):1673-1673.

199. Barraza RA, McLaren JW, Poeschla EM. Prostaglandin pathway gene therapy for sustained reduction of intraocular pressure. *Molecular therapy : the journal of the American Society of Gene Therapy.* 2010;18(3):491-501.

200. Khare PD, Loewen N, Teo W, et al. Durable, safe, multi-gene lentiviral vector expression in feline trabecular meshwork. *Molecular therapy : the journal of the American Society of Gene Therapy.* 2008;16(1):97-106.

201. Borrás T, Buie LK, Spiga MG. Inducible scAAV2.GRE.MMP1 lowers IOP long-term in a large animal model for steroid-induced glaucoma gene therapy. *Gene Ther.* 2016;23(5):438-449.

202. Huang AJ. Suppression of keratoepithelin and myocilin by small interfering RNA (an American Ophthalmological Society thesis). *Trans Am Ophthalmol Soc.* 2007;105:365-378.

203. Demetriades AM. Gene therapy for glaucoma. *Curr Opin Ophthalmol.* 2011;22(2):73-77.

204. Jinek M, Chylinski K, Fonfara I, Hauer M, Doudna JA, Charpentier E. A programmable dual-RNA-guided DNA endonuclease in adaptive bacterial immunity. *Science.* 2012;337(6096):816-821.

205. Zhu W, Gramlich OW, Laboissonniere L, et al. Transplantation of iPSC-derived TM cells rescues glaucoma phenotypes in vivo. *Proc Natl Acad Sci U S A.* 2016;113(25):E3492-3500.